ACKNOWLEDGMENTS. This study was supported in part by a grant for Research on Human Genome Tailor-Made from the Ministry of Health, Labor, and Welfare of Japan; Grants-in-Aid for Scientific Research (B) from the Japan Society for the Promotion of Science; and grants from The Yasuda Medical Foundation, The Sagawa Foundation for Promotion of Cancer Research, and The Mitsubishi Foundation.

1. Druker BJ, et al.; IRIS Investigators (2006) Five-year follow-up of patients receiving imatinib for chronic myeloid leukemia. *N Engl J Med* 355(23):2408–2417.
2. Soda M, et al. (2007) Identification of the transforming *EML4-ALK* fusion gene in non-small-cell lung cancer. *Nature* 448(7153):561–566.
3. Shaw AT, et al. (2011) Effect of crizotinib on overall survival in patients with advanced non-small-cell lung cancer harbouring ALK gene rearrangement: A retrospective analysis. *Lancet Oncol* 12(11):1004–1012.
4. Colicelli J (2004) Human RAS superfamily proteins and related GTPases. *Sci STKE* 2004 (250):RE13.
5. Cox AD, Der CJ (2010) Ras history: The saga continues. *Small GTPases* 1(1):2–27.
6. Jaffee EM, Hruban RH, Canto M, Kern SE (2002) Focus on pancreas cancer. *Cancer Cell* 2(1):25–28.
7. Wertheimer E, et al. (2012) Rac signaling in breast cancer: A tale of GEFs and GAPs. *Cell Signal* 24(2):353–362.
8. Ridley AJ, Paterson HF, Johnston CL, Diekmann D, Hall A (1992) The small GTP-binding protein rac regulates growth factor-induced membrane ruffling. *Cell* 70(3):401–410.
9. Qiu RG, Chen J, Kirn D, McCormick F, Symons M (1995) An essential role for Rac in Ras transformation. *Nature* 374(6521):457–459.
10. Senger DL, et al. (2002) Suppression of Rac activity induces apoptosis of human glioma cells but not normal human astrocytes. *Cancer Res* 62(7):2131–2140.
11. Thomas EK, et al. (2007) Rac guanosine triphosphatases represent integrating molecular therapeutic targets for BCR-ABL-induced myeloproliferative disease. *Cancer Cell* 12(5):467–478.
12. Rasheed S, Nelson-Rees WA, Toth EM, Arnstein P, Gardner MB (1974) Characterization of a newly derived human sarcoma cell line (HT-1080). *Cancer* 33(4):1027–1033.
13. Ueno T, et al. (2012) High-throughput resequencing of target-captured cDNA in cancer cells. *Cancer Sci* 103(1):131–135.
14. Hall A, Marshall CJ, Spurr NK, Weiss RA (1983) Identification of transforming gene in two human sarcoma cell lines as a new member of the ras gene family located on chromosome 1. *Nature* 303(5916):396–400.
15. Debnath J, Muthuswamy SK, Brugge JS (2003) Morphogenesis and oncogenesis of MCF-10A mammary epithelial acini grown in three-dimensional basement membrane cultures. *Methods* 30(3):256–268.
16. Hill CS, Wynne J, Treisman R (1995) The Rho family GTPases RhoA, Rac1, and CDC42Hs regulate transcriptional activation by SRF. *Cell* 81(7):1159–1170.
17. Marshall CJ, Hall A, Weiss RA (1982) A transforming gene present in human sarcoma cell lines. *Nature* 299(5879):171–173.
18. Adari H, Lowy DR, Willumsen BM, Der CJ, McCormick F (1988) Guanosine triphosphatase activating protein (GAP) interacts with the p21 ras effector binding domain. *Science* 240(4851):518–521.
19. Calés C, Hancock JF, Marshall CJ, Hall A (1988) The cytoplasmic protein GAP is implicated as the target for regulation by the ras gene product. *Nature* 332(6164): 548–551.
20. Reinstein J, Schlichting I, Frech M, Goody RS, Wittinghofer A (1991) p21 with a phenylalanine 28——leucine mutation reacts normally with the GTPase activating protein GAP but nevertheless has transforming properties. *J Biol Chem* 266(26): 17700–17706.
21. Lin R, Bagrodia S, Cerione R, Manor D (1997) A novel Cdc42Hs mutant induces cellular transformation. *Curr Biol* 7(10):794–797.
22. Krauthammer M, et al. (2012) Exome sequencing identifies recurrent somatic RAC1 mutations in melanoma. *Nat Genet* 44(9):1006–1014.
23. Paterson H, et al. (1987) Activated N-ras controls the transformed phenotype of HT1080 human fibrosarcoma cells. *Cell* 51(5):803–812.
24. Hodis E, et al. (2012) A landscape of driver mutations in melanoma. *Cell* 150(2): 251–263.

Published OnlineFirst May 2, 2012; DOI:10.1158/1078-0432.CCR-11-2972

Clinical Cancer Research

Cancer Therapy: Preclinical

Paracrine Receptor Activation by Microenvironment Triggers Bypass Survival Signals and ALK Inhibitor Resistance in EML4-ALK Lung Cancer Cells

Tadaaki Yamada[1], Shinji Takeuchi[1], Junya Nakade[1], Kenji Kita[1], Takayuki Nakagawa[1,2], Shigeki Nanjo[1], Takahiro Nakamura[3], Kunio Matsumoto[3], Manabu Soda[4], Hiroyuki Mano[4], Toshimitsu Uenaka[2], and Seiji Yano[1]

Abstract

Purpose: Cancer cell microenvironments, including host cells, can critically affect cancer cell behaviors, including drug sensitivity. Although crizotinib, a dual tyrosine kinase inhibitor (TKI) of ALK and Met, shows dramatic effect against *EML4-ALK* lung cancer cells, these cells can acquire resistance to crizotinib by several mechanisms, including ALK amplification and gatekeeper mutation. We determined whether microenvironmental factors trigger ALK inhibitor resistance in *EML4-ALK* lung cancer cells.

Experimental Design: We tested the effects of ligands produced by endothelial cells and fibroblasts, and the cells themselves, on the susceptibility of *EML4-ALK* lung cancer cell lines to crizotinib and TAE684, a selective ALK inhibitor active against cells with *ALK* amplification and gatekeeper mutations, both *in vitro* and *in vivo*.

Results: *EML4-ALK* lung cancer cells were highly sensitive to ALK inhibitors. EGF receptor (EGFR) ligands, such as EGF, TGF-α, and HB-EGF, activated EGFR and triggered resistance to crizotinib and TAE684 by transducing bypass survival signaling through Erk1/2 and Akt. Hepatocyte growth factor (HGF) activated Met/Gab1 and triggered resistance to TAE684, but not crizotinib, which inhibits Met. Endothelial cells and fibroblasts, which produce the EGFR ligands and HGF, respectively, decreased the sensitivity of *EML4-ALK* lung cancer cells to crizotinib and TAE684, respectively. EGFR-TKIs resensitized these cells to crizotinib and Met-TKI to TAE684 even in the presence of EGFR ligands and HGF, respectively.

Conclusions: Paracrine receptor activation by ligands from the microenvironment may trigger resistance to ALK inhibitors in *EML4-ALK* lung cancer cells, suggesting that receptor ligands from microenvironment may be additional targets during treatment with ALK inhibitors. *Clin Cancer Res; 18(13); 3592–602. ©2012 AACR.*

Introduction

ALK fusion with EML4 in non–small cell lung cancer (NSCLC) was first detected in 2007 (1), with 3% to 7% of unselected NSCLCs having this fusion gene (1–4). EML4-ALK lung cancer is more frequently observed in patients with adenocarcinoma than with other histologies, in young adults than in older patients, and in never-smokers or light smokers (<15 pack-years) than in heavier smokers (2, 3). ALK kinase inhibitors show dramatic effects against lung cancers with *EMK4-ALK in vitro* and *in vivo* (3, 4). In a phase I–II trial with crizotinib, a dual tyrosine kinase inhibitor (TKI) of ALK and Met, the overall response rate was 47 of 82 (57%) patients with *EML4-ALK*–positive tumors (5). However, almost all patients who show a marked response to ALK-TKIs acquire resistance to these agents after varying periods of time (6, 7). Secondary mutations, including the gatekeeper L1196M mutation and others (F1174L, C1156Y, G1202R, S1206Y, 1151-T-ins, and G1269A), *ALK* amplification, *KIT* amplification, and autophosphorylation of EGF receptor (EGFR), were shown to be responsible for acquired resistance to crizotinib in ALK-translocated cancers (6–10).

Selective ALK inhibitors, including TAE684 and CH5424802, have been reported active against *EML4-ALK* lung cancer cells with *ALK* amplification and secondary mutations. These cells, however, may develop resistance to this class of inhibitor, due to several mechanisms, including novel *ALK* mutations (L1152R, L1198P, and D1203N), coactivation of EGFR and ErbB2, and EGFR phosphorylation (3, 11, 12).

Authors' Affiliations: [1]Division of Medical Oncology, Cancer Research Institute, Kanazawa University, Kanazawa, Ishikawa; [2]Tsukuba Research Laboratories, Eisai co., ltd., Ibaraki; [3]Division of Tumor Dynamics and Regulation, Cancer Research Institute, Kanazawa University, Kanazawa, Ishikawa; and [4]Division of Functional Genomics, Jichi Medical University, Shimotsuke, Tochigi, Japan

Note: Supplementary data for this article are available at Clinical Cancer Research Online (http://clincancerres.aacrjournals.org/).

Corresponding Author: Seiji Yano, Division of Medical Oncology, Cancer Research Institute, Kanazawa University 13-1, Takara-machi, Kanazawa, Ishikawa 920-0934, Japan. Phone: 81-76-265-2794; Fax: 81-76-234-4524; E-mail: syano@staff.kanazawa-u.ac.jp

doi: 10.1158/1078-0432.CCR-11-2972

Published OnlineFirst May 2, 2012; DOI:10.1158/1078-0432.CCR-11-2972

Translational Relevance

Although crizotinib, a dual inhibitor of ALK and Met, shows dramatic effects against *EML4-ALK* lung cancer cells, these cells can acquire resistance by several mechanisms, including ALK amplification and gatekeeper mutation. Selective ALK inhibitors may overcome crizotinib resistance due to these mechanisms, but these cells may become resistant to these inhibitors.

We show here that EGF receptor ligands produced by endothelial cells can cause *EML4-ALK* lung cancer cells to become resistant to crizotinib and selective ALK inhibitors by triggering bypass survival signals. By contrast, hepatocyte growth factor produced by fibroblasts can induce resistance to selective ALK inhibitors, but not crizotinib. Because endothelial cells and fibroblasts are components of the microenvironment, our findings raise clinical questions about the class of ALK inhibitors more beneficial for *EML4-ALK* lung cancer patients. Moreover, our results provide a rationale for targeting receptor ligands in the microenvironment for more successful treatment with ALK inhibitors.

Most human cancers are composed of cancer cells that coexist with a variety of extracellular matrix components and cell types, including fibroblasts, endothelial cells, and immune cells, which collectively form the tumor microenvironment (13). This microenvironment can influence the growth, survival, invasiveness, metastatic ability, and drug sensitivity of cancer cells within these tumors (14). Paracrine signaling between cancer cells and host cells in the microenvironment, mediated by cytokines, chemokines, growth factors, and other signaling molecules, plays a critical role in tumor growth (15). As receptors for these factors, the EGFR family of receptors and Met are of particular interest in lung cancer (16). The EGFR family consists of at least 4 receptor tyrosine kinases, including EGFR (ErbB1), Her2/neu (ErbB2), HER3 (ErbB3), and HER4 (ErbB4). To date, 7 ligands for EGFR have been identified: EGF, TGF-α; heparin-binding EGF-like growth factor (HB-EGF); amphiregulin; betacellurin; epiregulin; and epigen (17). By contrast, Met is the only specific receptor for hepatocyte growth factor (HGF) and HGF binds only to Met (18). Many lung cancer cells express EGFR and Met, with these cells and others in their microenvironment expressing their ligands (19, 20), suggesting that these receptors and ligands modulate the sensitivity of cancer cells to molecular targeted drugs in their microenvironment. We previously showed that fibroblast-derived HGF induces EGFR-TKI resistance in *EGFR*-mutant lung cancer cells by activating Met and downstream pathways (21, 22). However, the role of the microenvironment in the sensitivity of EML4-ALK lung cancer cells to ALK-TKIs has not been determined. We therefore examined whether factors in the microenvironment of *EML4-ALK* lung cancer cells trigger their resistance to crizotinib and TAE684, a selective ALK inhibitor, as well as clarifying their underlying mechanisms of action.

Materials and Methods

Cell culture

The H2228 human lung adenocarcinoma cell line, with the EML4-ALK fusion protein variant3 (E6;A20), the umbilical vein endothelial cell line human umbilical vein endothelial cells (HUVEC) and the human bronchial epithelial cell line BEAS-2B, transformed with SV40 virus, were purchased from the American Type Culture Collection. The H3122 human lung adenocarcinoma cell line, with the EML4-ALK fusion protein variant1 (E13;A20), was kindly provided by Dr. Jeffrey A. Engelman of the Massachusetts General Hospital Cancer Center, Boston, MA (3). The MANA2 mouse lung adenocarcinoma cell line was established in Jichi Medical University from a tumor nodule developed in a transgenic mouse expressing *EML4-ALK* variant 1 (E13;A20) (23). The MRC-5 and IMR-90 lung embryonic fibroblast cell lines were obtained from RIKEN Cell Bank. The human dermal microvessel endothelial cell line HMVEC was purchased from Kurabo. The monocytic leukemia cell line U937 was purchased from Health Science Research Resources Bank. H2228 cells were cultured in RPMI-1640 medium, MANA2 cells were cultured in DMEM/F12+GlutaMAX-1, and MRC-5 (P 25–30) cells were cultured in Dulbecco's modified Eagle's medium (DMEM) medium, supplemented with 5% fetal bovine serum, penicillin (100 U/mL), and streptomycin (50 μg/mL), in a humidified CO_2 incubator at 37°C. HMVECs and HUVECs were maintained in HuMedia-MvG with growth supplements (Kurabo) and used for *in vitro* assays at passages 2 to 5 and 2 to 4, respectively. BEAS-2B cells were maintained in LHC9/RPMI-1640 medium, as described (24), and used for *in vitro* assays at passages 42 to 46. Macrophage differentiation of U937 cells was induced by incubation in RPMI-1640 medium containing 10 ng/mL phorbol 12-myristate 13-acetate (Sigma Chemical Co.; ref. 25) for 5 days, with floating cells removed by rinsing with PBS, as described (26). Differentiated U937 cells (PMA-U937 cells) attached to the dishes were used for *in vitro* assays at passages 6 to 8. All cells were passaged for less than 3 months before renewal from frozen, early-passage stocks obtained from the indicated sources. Cells were regularly screened for *Mycoplasma* using a MycoAlert *Mycoplasma* Detection Kit (Lonza).

Reagents

TAE684, crizotinib, and WZ4002 were purchased from Seleck Chemicals. Erlotinib hydrochloride was obtained from Chugai Pharmaceutical Co., Ltd. The anti-human EGFR antibody cetuximab was obtained from Merck Serono. E7050 was synthesized by Eizai Co., Ltd. (27). Goat anti-human HGF antibody, control goat IgG, recombinant EGF, TGF-α, HB-EGF, IGF-1, and PDGF-AA were purchased from R&D Systems. Recombinant HGF was prepared as described (28).

Published OnlineFirst May 2, 2012; DOI:10.1158/1078-0432.CCR-11-2972

Cell growth assay

Cell proliferation was measured using the MTTdye reduction method (17). Tumor cells at 80% confluence were harvested, seeded at 2×10^3 cells per well in 96-well plates, and incubated in appropriate medium for 24 hours. Several concentrations of TAE684, crizotinib, erlotinib, WZ4002, E7050, cetuximab, anti-HGF antibody, and/or EGF, TGF-α, HB-EGF, IGF-1, PDGF-AA, and HGF were added to each well, and incubation was continued for a further 72 hours. To each well was added 50 μL MTT (2 mg/mL; Sigma), followed by incubation for 2 hours at 37°C. The media were removed and the dark blue crystals in each well were dissolved in 100 μL of dimethyl sulfoxide (DMSO). Absorbance was measured with an MTP-120 Microplate reader (Corona Electric) at test and reference wavelengths of 550 and 630 nm, respectively. The percentage growth was calculated relative to untreated controls. Each assay was carried out at least in triplicate, with results based on 3 independent experiments.

Apoptosis assay

H2228 and H3122 cells (3×10^3 cells) were seeded in 96-well, white-walled plates and incubated overnight. The cells were treated with crizotinib (1 μmol/L) or vehicle (DMSO) for 48 hours. Cellular apoptosis was determined by measuring caspase-3/7 activity using a luminometric Caspase-Glo 3/7 assay (Promega) according to the manufacturer's protocol, with luminescence intensity measured using a Fluoroskan Ascent FL plate reader (Thermo Scientific). Cellular apoptosis was expressed relative to DMSO-treated control cells.

RNA interference

Duplexed Stealth RNAi (Invitrogen) against *EGFR*, *Met*, *ErbB3*, *Gab1*, *ALK*, and Stealth RNAi-negative control low GC Duplex #3 (Invitrogen) were used for RNA interference (RNAi) assays. Briefly, aliquots of 1×10^5 cells in 2 mL of antibiotic-free medium were plated into each well of a 6-well plate and incubated at 37°C for 24 hours. The cells were transfected with siRNA (250 pmol) or scrambled RNA using Lipofectamine 2000 (5 μL) in accordance with the manufacturer's instructions (Invitrogen). After 24 hours, the cells were washed twice with PBS and incubated with or without crizotinib (100 nmol/L), TAE684 (100 nmol/L), recombinant human EGF (100 ng/mL), TGF-α (100 ng/mL), HB-EGF (10 ng/mL), or HGF (50 ng/mL) for an additional 48 hours in antibiotic-containing medium. These tumor cells were then used for cell proliferation assays, with *EGFR*, *Met*, *ErbB3*, *Gab1*, and *ALK* knockdowns (#1, #2) confirmed by Western blotting.

The siRNA target sequences were as follows: *EGFR*, 5′-CGGAATAGGTATTGGTGAATTTAAA-3′ and 5′-UUUAAAUUCACCAAUACCUAUUCCG-3′, *Met*, 5′-UCCAGAAGAUCAGUUUCCUAAUUCA-3′ and 5′-UGAAUUAGGAAACUGAUCUUCUGGA-3′, *ErbB3*, 5′-GGCCAUGAAUGAAUUCUCUACUCUA-3′ and 5′-UAGAGUAGAGAAUUCAUUCAUGGCC-3′, *Gab1*, 5′-UAGAGUAGCAGAGGAUGAAUCUGCC-3′ and 5′-GGCAGAUUCAUCCUCUGCUACUCUA-3′, *ALK #1*, 5′-UCAUUAUCCGGUAUACAGGCCCAGG-3′ and 5′-CCUGGGCCUGUAUACCGGAUAAUGA-3′, and ALK #2, 5′-AAAGCUGCACUCCAGACCAUAUCGG-3′ and 5′-CCGAUAUGGUCUGGAGUGCAGCUUU-3′. Each assay was carried out at least in triplicate, with 3 independent experiments conducted.

Western blotting

SDS polyacrylamide gels (Bio-Rad) were loaded with 40 μg total protein per lane; following electrophoresis, the proteins were transferred onto polyvinylidene difluoride membranes (Bio-Rad), which were incubated with Blocking One (Nacalai Tesque) for 1 hour at room temperature, followed by overnight incubation at 4°C with anti-ALK (C26G7), anti–phospho-ALK (Tyr1604), anti–phospho-EGFR (Tyr1068), anti-STAT-3(79D7), anti–phospho-STAT-3 (Y705), anti-Akt, anti–phospho-Akt (Ser473), anti-ErbB4 (111B2), anti–phospho-ErbB4 (Tyr1284), anti-Met (25H2), anti–phospho-Met (Y1234/Y1235) (3D7), anti-Gab1 (#3232), anti-phospho-Gab1 (Tyr627) (C32H2), anti-ErbB3 (1B2), anti–phospho-ErbB3 (Tyr1289) (21D3), or anti-β-actin (13E5) antibodies (1:1,000 dilution each; Cell Signaling Technology), or with anti-human EGFR (1 μg/mL), anti-human/mouse/rat extracellular signal-regulated kinase (Erk)1/Erk2 (0.2 μg/mL), or anti-phospho-Erk1/Erk2 (T202/Y204) (0.1 μg/mL) antibodies (R&D Systems). After washing 3 times, the membranes were incubated for 1 hour at room temperature with secondary Ab (horseradish peroxidase–conjugated species-specific Ab). Immunoreactive bands were visualized with SuperSignal West Dura Extended Duration Substrate Enhanced Chemiluminescent Substrate (Pierce). Each experiment was carried out at least 3 times independently.

HGF, EGF, TGF-α, and HB-EGF production in cell culture supernatant

Cells (2×10^5) were cultured in 2 mL of RPMI-1640 or DMEM with 5% FBS for 24 hours. The cells were washed with PBS and incubated for 48 hours in RPMI-1640 or DMEM with 5% FBS. The culture medium was harvested and centrifuged, and the supernatant was stored at −70°C until analysis. HGF (Immunis HGF EIA; B-Bridge International), EGF, TGF-α, and HB-EGF (Quantikine ELISA kits; R&D Systems) were assayed by ELISA, in accordance with the manufacturer's procedures. All samples were run in triplicate. Color intensity was measured at 450 nm with a spectrophotometric plate reader. Growth factor concentrations were determined by comparison with standard curves. The detection limits for HGF, EGF, TGF-α, and HB-EGF were 0.1 ng/mL, 3.9 pg/mL, 15.6 pg/mL, and 31.2 pg/mL, respectively.

Coculture of lung cancer cells with fibroblasts or endothelial cells

Cells were cocultured in Transwell Collagen–Coated chambers separated by an 8-μm (BD Biosciences, Erembodegem) or 3-μm (Corning Costar) pore size filter. Tumor cells (8×10^3 cells/800 μL) with or without TAE684

Published OnlineFirst May 2, 2012; DOI:10.1158/1078-0432.CCR-11-2972

(100 nmol/L) or crizotinib (100 nmol/L) in the lower chamber were cocultured with MRC-5 (1×10^4 cells/300 μL) or HMVEC (1×10^4 cells/300 μL) cells, with or without 2 hours of pretreatment with anti-human HGF antibody (2 μg/mL) or cetuximab (2 μg/mL) in the upper chamber for 72 hours. The upper chamber was then removed, 200 μL of MTT solution (2 mg/mL; Sigma) was added to each well and the cells were incubated for 2 hours at 37°C. The media were removed and the dark blue crystals in each well were dissolved in 400 μL of DMSO. Absorbance was measured with an MTP-120 Microplate reader (Corona Electric) at test and reference wavelengths of 550 and 630 nm, respectively. The percentage growth was measured relative to untreated controls. All samples were assayed at least in triplicate, with each experiment conducted 3 times independently.

Xenograft studies in SCID mice

Suspensions of H2228 cells (5×10^6), with or without MRC-5 cells (5×10^6), were injected subcutaneously into the backs of 5-week-old male severe combined immunodeficient (SCID) mice (Japan Clea). After 4 days (tumors diameter >4 mm), mice were randomly allocated into groups of 6 animals to receive TAE684 (1.25 mg/kg/d) or vehicle by oral gavage. Tumor size was measured with digital calipers, and tumor volume was calculated as 0.5 × length × (width)^2. All animal experiments complied with the Guidelines for the Institute for Experimental Animals, Kanazawa University Advanced Science Research Center (approval no. AP-081088).

HGF production in tumor tissues

Tumors obtained from SCID mice after 4 and 8 days were lysed in mammalian tissue lysis buffer containing a phosphatase and proteinase inhibitor cocktail (Sigma). HGF was quantitated by ELISA (Immunis HGF EIA; Institute of Immunology), with a detection limit of 0.1 ng/mL. All samples were assayed in triplicate.

Statistical analysis

Differences were analyzed by one-way ANOVA. All statistical analyses were carried out using GraphPad Prism Ver. 4.01 (GraphPad Software, Inc.). $P < 0.05$ was considered significant.

Results

HGF and/or EGFR ligands reduced the sensitivity of EML4-ALK lung cancer cells to ALK inhibitor *in vitro*

We first examined the sensitivity of human H2228, human H3122, and mouse MANA2 lung cancer cell lines, all containing EML4-ALK translocations, to the ALK inhibitors crizotinib and TAE684, and to various EGFR-TKIs. Human H2228 cells with *EML4-ALK* variant 3 (E6;A20) and H3122 cells with *EML4-ALK* variant 1 (E13;A20) were insensitive to the EGFR-TKIs erlotinib (a reversible EGFR-TKI) and WZ4002 (selective for mutant EGFR), but sensitive to the ALK-TKIs crizotinib and TAE684 (Fig. 1). MANA2 cells, established from lung tumors of an *EML4-ALK* variant 1 (E13;A20) transgenic mouse, were also sensitive to crizotinib and TAE684, although their viability was slightly inhibited by high concentrations (1 μmol/L) of EGFR-TKIs.

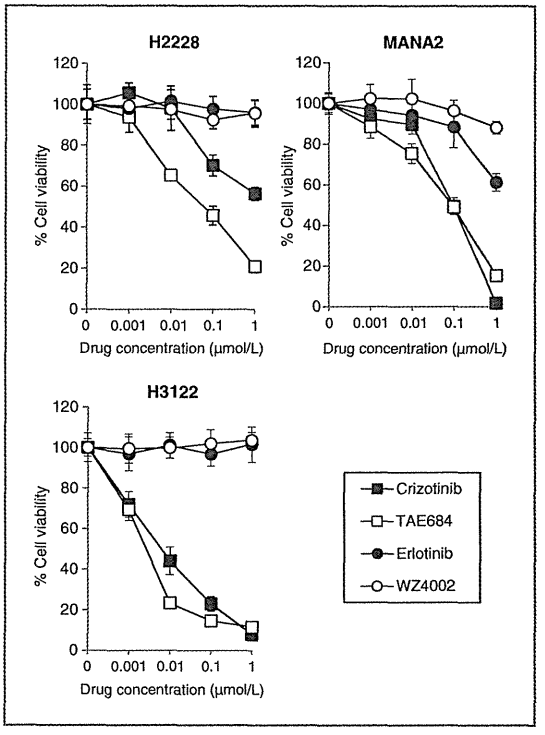

Figure 1. EML4-ALK lung cancer cells are highly sensitive to the ALK inhibitors, crizotinib, and TAE684. The sensitivity of EML4-ALK lung cancer cells, human H2228, human H3122, and mouse MANA2, to the ALK inhibitors, crizotinib, and TAE684 were determined by analyzing the effects of the EGFR-TKIs, erlotinib (reversible EGFR-TKI), and WZ4002 (mutant EGFR selective TKI). Tumor cell growth after 72 hours was measured by the MTT assay. Each sample was assayed in triplicate, with each experiment repeated at least 3 times independently.

Because several growth factors have been associated with poor patient prognosis and/or drug resistance in lung cancer, we explored the effect of EGFR ligands (EGF, TGF-α, and HB-EGF), IGF-1, PDGF-AA, and HGF on the sensitivity of *EML4-ALK* lung cancer cells to ALK inhibitors. In the absence of ALK inhibitors, these growth factors slightly increased the viability of H2228, H3122, and MANA2 cells. In H2228 cells, all 3 EGFR ligands reduced sensitivity to crizotinib in a dose-dependent manner, but IGF-1, PDGF-AA, and HGF failed to do so (Fig. 2, Supplementary Fig. S1). Interestingly, HGF, as well as the EGFR ligands, reduced sensitivity to TAE684, but IGF-1 and PDGF-AA failed to do so. Similar results were observed in H3122 and MANA2 cells. To further confirm the effect of these growth factors on specific ALK inhibition, we knocked down ALK using 2 different specific siRNAs in H2228 cells. Whereas H2228 cells were highly sensitive to *ALK*-specific siRNAs, EGFR ligands and HGF restored cell viability inhibited by ALK knockdown (Supplementary Fig. S2). When we

Published OnlineFirst May 2, 2012; DOI:10.1158/1078-0432.CCR-11-2972

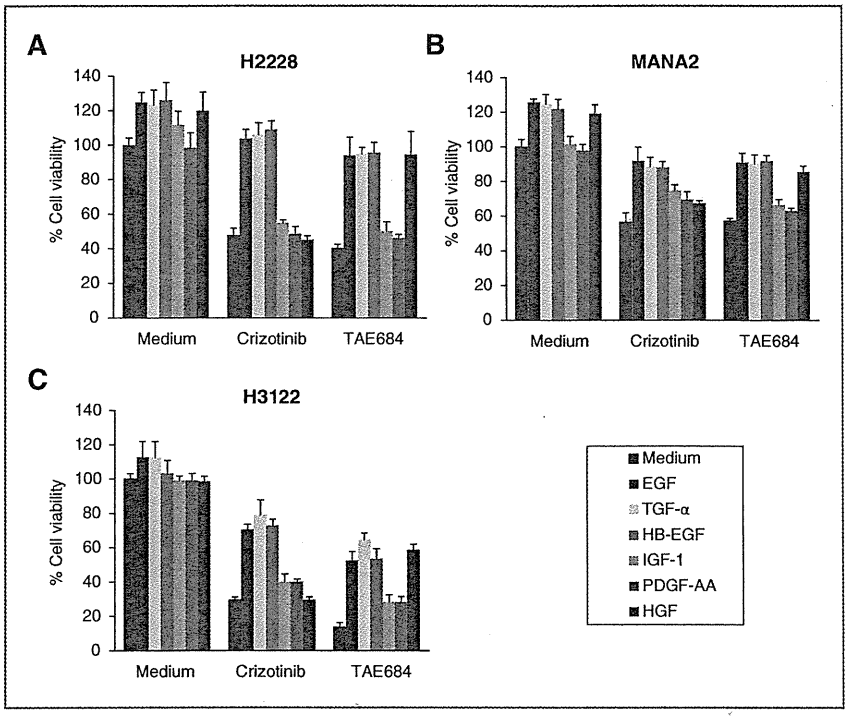

Figure 2. HGF and/or EGFR ligands (EGF, TGF-α, and HB-EGF) reduce the sensitivity of EML4-ALK lung cancer cells to ALK inhibitors *in vitro*. H2228, H3122, and MANA2 cells were incubated with or without crizotinib (100 nmol/L), TAE684 (100 nmol/L), and/or EGF, TGF-α, IGF-I, or PDGF-AA (100 ng/mL); HB-EGF (10 ng/mL), or HGF (50 ng/mL), with cell growth determined after 72 hours. The percentage growth is shown relative to untreated controls. Each sample was assayed in triplicate, with each experiment repeated at least 3 times independently.

assessed the ability of crizotinib to induce apoptosis in H2228 and H3122 cells, we found that crizotinib induced apoptosis in H3122, but not H2228, cells (Supplementary Fig. S3).

HGF and EGFR ligands trigger ALK inhibitor resistance via Met and EGFR, respectively

To assess the mechanism by which these growth factors reduced cell sensitivity to ALK inhibitors, we analyzed the phosphorylation status of ALK, receptors, and their downstream molecules in H2228, H3122, and MANA2 cells by Western blotting. Crizotinib inhibited ALK phosphorylation, thereby suppressing the phosphorylation of Akt, Erk1/2 and STAT-3, as described (ref. 11; Fig. 3A, Supplementary Fig. S4). The EGFR ligands, EGF, TGF-α, and HB-EGF stimulated EGFR phosphorylation. Crizotinib inhibited ALK and STAT-3 phosphorylation even in the presence of EGFR ligands, but failed to inhibit phosphorylation of EGFR and downstream Akt, and Erk1/2. Phosphorylation of ErbB4, a potential receptor for HB-EGF, was not affected by crizotinib or EGFR ligands. To further confirm the involvement of EGFR in crizotinib resistance induced by EGFR ligands, we knocked down EGFR by specific siRNAs in H2228 and H3122 cells (Fig. 3B). Although crizotinib markedly inhibited cell viability and all 3 EGFR ligands induced resistance in cells treated with scrambled siRNA, resistance to crizotinib was not induced by EGF, TGF-α, or HB-EGF in EGFR siRNA-treated cells, indicating that EGFR ligand-triggered crizotinib resistance is mediated by EGFR.

In parallel experiments, TAE684 inhibited ALK phosphorylation, thereby suppressing the phosphorylation of Akt, Erk1/2, and STAT-3 (Fig. 3C). HGF stimulated the phosphorylation of Met and its adaptor protein, Gab1, as described (29). TAE684 inhibited ALK and STAT-3 phosphorylation even in the presence of HGF, but failed to inhibit phosphorylation of Met and downstream Akt and Erk1/2. Phosphorylation of ErbB3, an adaptor of amplified, but not HGF-stimulated Met (30), was not affected by TAE684 or HGF. To further confirm the involvement of Met and Gab1 in HGF-induced TAE684 resistance, we knocked down Met, ErbB3, or Gab1 by specific siRNAs in H2228 and H3122 cells (Fig. 3D). TAE684 markedly inhibited the viability and HGF induced resistance in cells treated with scrambled siRNA. Importantly, treatment of cells with Met or Gab1, but not ErbB3, siRNA, induced TAE684 resistance, indicating the involvement of Met/Gab1 in HGF-induced resistance to TAE684.

Cross-talk of endothelial cells and fibroblasts reduces the sensitivity of EML4-ALK lung cancer cells to ALK inhibitors

To determine which types of host cells could produce EGFR ligands and HGF, we investigated production of these growth factors by various types of host stromal cells, comparing lung epithelial cells and cancer cells. The endothelial cell lines HMVEC produced discernible levels of EGFR ligands, including EGF, TGF-α, and HB-EGF, whereas fibroblasts produced a high level of HGF (Fig. 4A). EML4-ALK lung cancer cells (H2228, H3122, and

Published OnlineFirst May 2, 2012; DOI:10.1158/1078-0432.CCR-11-2972

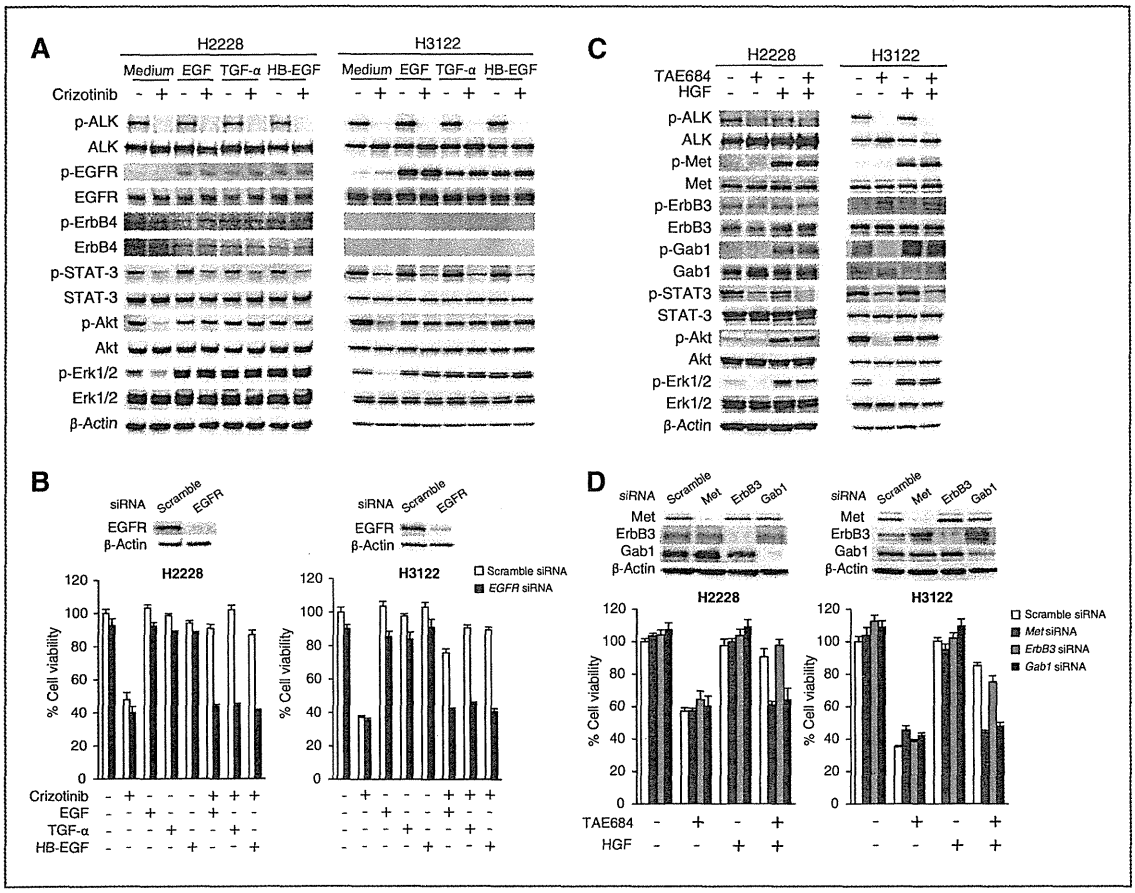

Figure 3. HGF and EGFR ligands trigger ALK inhibitor resistance via Met/Gab1 and EGFR, respectively. A, crizotinib inhibited the phosphorylation of ALK and STAT-3 but not that of EGFR, Akt, and Erk1/2 in the presence of EGF, TGF-α, or HB-EGF. Tumor cells were treated with or without crizotinib (100 nmol/L) for 1 hour and/or EGF (100 ng/mL), TGF-α (100 ng/mL), or HB-EGF (10 ng/mL) for 15 minutes. The cells were lysed and the indicated proteins were detected by immunoblotting. The results shown are representative of 3 independent experiments. B, control or *EGFR*-specific siRNAs were introduced into H2228 and H3122 cells. After 24 hours, the cells were incubated with or without crizotinib (100 nmol/L), and/or EGF (100 ng/mL), TGF-α (100 ng/mL), or HB-EGF (10 ng/mL) for 72 hours and lung cancer cell growth was determined by MTT assays. *EGFR* knockdown was confirmed by immunoblotting. The percentage of growth is shown relative to untreated controls. Each sample was assayed in triplicate, with each experiment repeated at least 3 times independently. C, TAE684 inhibited the phosphorylation of ALK and STAT-3, but not that of Met, Gab1, Akt, and Erk1/2 in the presence of HGF. Tumor cells were treated with or without TAE684 (100 nmol/L) for 1 hour and/or HGF (50 ng/mL) for 15 minutes. The cells were lysed and the indicated proteins were detected by immunoblotting. The results shown are representative of 3 independent experiments. D, control or *Met*, *ErbB3*, or *Gab1*-specific siRNAs were introduced into H2228 and H3122 cells. After 24 hours, the cells were incubated with or without TAE684 (100 nmol/L) and/or HGF (50 ng/mL) for 72 hours and lung cancer cell growth was determined by MTT assays. *Met*, *Gab1*, and *ErbB3* knockdowns were confirmed by immunoblotting. The percentage of growth is shown relative to untreated controls. Each sample was assayed in triplicate, with each experiment repeated at least 3 times independently.

MANA2) and lung epithelial cells (BEAS-2B) produced low or no detectable levels of EGFR ligands or HGF. Interestingly, coculture of H2228 or H3122 cells with fibroblasts (MRC-5) significantly reduced their sensitivity to TAE684, an effect abrogated by anti-HGF antibody (Fig. 4B). Coculture with endothelial cells (HMVEC) also reduced sensitivity to crizotinib, an effect inhibited by anti-EGFR antibody (Fig. 4C).

These results suggested that host stromal cells, such as endothelial cells and fibroblasts, may regulate sensitivity to ALK inhibitors by secreting EGFR ligands and HGF, respectively.

HGF derived from fibroblasts induces TAE684 resistance of EML4-ALK lung cancer cells *in vivo*

To investigate whether sensitivity to TAE684 could be affected by fibroblasts *in vivo*, we subcutaneously inoculated H2228 cells, with or without MRC-5 cells, into SCID mice. The tumors of mice injected with H2228 and MRC-5 cells grew slightly faster than those of mice injected with

Published OnlineFirst May 2, 2012; DOI:10.1158/1078-0432.CCR-11-2972

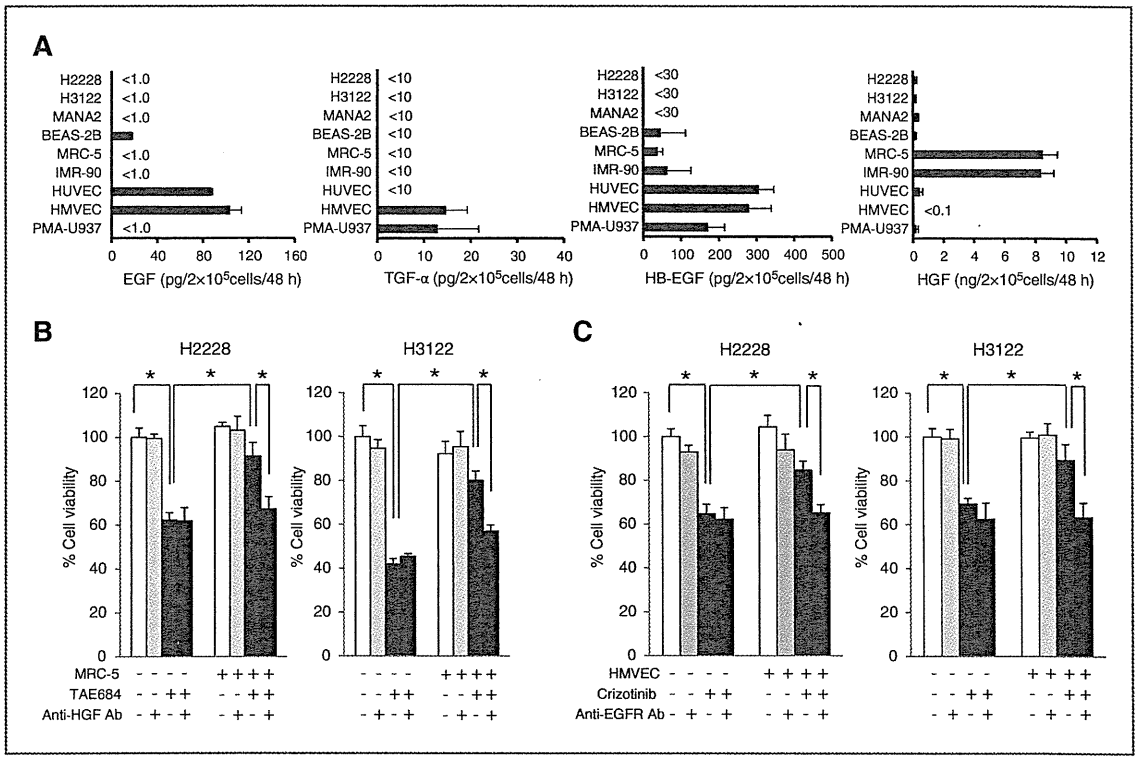

Figure 4. Cross-talk of endothelial cells and fibroblasts reduces sensitivity of EML4-ALK lung cancer cells to ALK inhibitors. A, receptor ligand production was assayed in lung cancer (H2228, H3122, and MANA2), human bronchial epithelial cell (BEAS-2B), fibroblasts (MRC-5 and IMR-90), endothelial cells (HUVEC and HMVEC), and the macrophage differentiated cell line (PMA-U937). The cells were incubated in medium for 48 hours, culture supernatants were harvested, and EGF, TGF-α, HB-EGF, and HGF concentrations were determined by ELISA. All samples were assayed in triplicate. B, H2228 and H3122 cells were cocultured with or without fibroblasts, MRC-5 cells, and/or anti-HGF–neutralizing antibody (2 μg/mL), in the presence or absence of TAE684 (100 nmol/L) for 72 hours, with cell growth determined by MTT assays. *, $P < 0.05$ (one-way ANOVA). Each experiment included triplicate determinations, and each experiment was repeated at least 3 times independently. C, endothelial cell–derived EGFR ligands induced crizotinib resistance in lung cancer cells with EML4-ALK fusion protein, an induction abrogated by blockade of EGFR. H2228 and H3122 cells were cocultured with or without endothelial cells, HMVECs, and/or anti-EGFR–neutralizing antibody (2 μg/mL) in the presence or absence of crizotinib (100 nmol/L) for 72 hours, with cell growth determined as in B. *, $P < 0.05$ (one-way ANOVA). Each experiment included triplicate determinations, with each experiment repeated at least 3 times independently.

H2228 cells alone, but the difference was not statistically significant by day 8 (Fig. 5A). TAE684 treatment, beginning on day 4, caused marked regression of tumors in mice injected with H2228 cells alone, but not of tumors in mice injected with H2228 and MRC-5 cells, indicating that fibroblasts induced resistance to TAE684 *in vivo* (Fig. 5A). We confirmed that HGF was produced by MRC-5 cells *in vivo*. Although the tumors of mice injected with H2228 cells alone did not produce detectable levels of HGF, the tumors of mice injected with H2228 and MRC-5 cells produced high levels of HGF, started on day 4, but decreasing slightly on day 8 (Fig. 5B).

We further analyzed whether coinjection of MRC-5 cells restored the Akt pathway inhibited by TAE684 in the tumors. Western blotting showed that TAE684 treatment inhibited Akt phosphorylation, which was restored by coinjection of MRC-5 cells (Fig. 5C). These results suggested that fibroblasts produced HGF in the tumors and restored Akt phosphorylation as a survival signal, as well as inducing resistance to TAE684 in EML4-ALK lung cancer cells *in vivo*.

Ligand-triggered resistance to ALK inhibitors is abrogated by inhibitors of both HGF-Met and EGFR

To establish novel strategies to treat EGFR ligand- or HGF-triggered resistance to ALK inhibitors, we examined the effect of combinations of ALK inhibitors with EGFR inhibitors (anti-EGFR Abs and reversible EGFR-TKIs) and HGF-Met inhibitors (anti-HGF Abs and Met-TKIs). Combined treatment with erlotinib, a reversible EGFR-TKI and cetuximab, an anti-EGFR Ab, successfully resensitized H2228 and H3122 cells to crizotinib even in the presence of the EGFR ligands, EGF (Fig. 6A), TGF-α (Fig. 6B), and HB-EGF (Fig. 6C). Moreover, the combination of HGF with E7050 (Met-TKI) or anti-HGF Ab resensitized cells to TAE684 (Fig. 6D).

Published OnlineFirst May 2, 2012; DOI:10.1158/1078-0432.CCR-11-2972

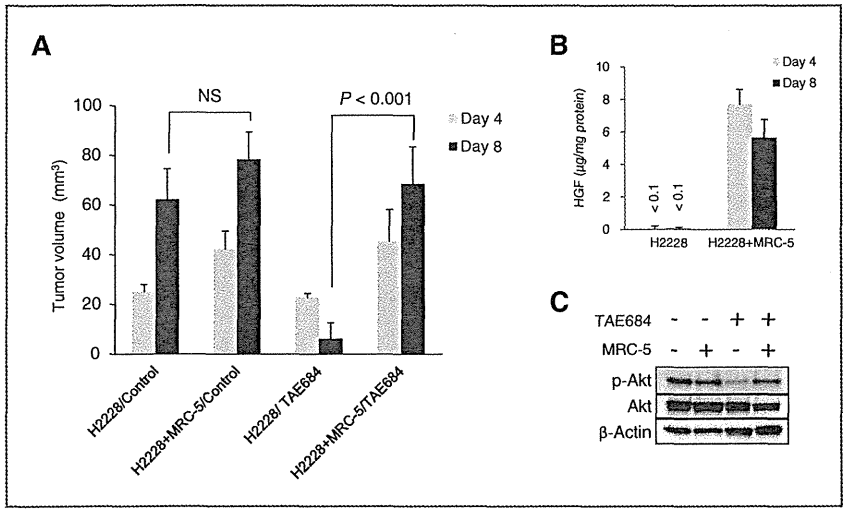

Figure 5. HGF derived from fibroblasts induces TAE684 resistance of EML4-ALK lung cancer cells *in vivo*. A, fibroblast-derived HGF induced TAE684 resistance in H2228 tumors in SCID mice. H2228 cells (5×10^6), with or without MRC-5 cells (5×10^6), were inoculated subcutaneously into SCID mice on day 0. Starting on day 4, mice received oral TAE684 (1.25 mg/kg/d) or vehicle alone, with tumor size measured on days 4 and 8. Tumor volumes were calculated as described in Materials and Methods. Data shown are the representative of 2 independent experiments. Error bars indicate SEs of 6 mice. $P < 0.05$ was considered significant by one-way ANOVA. NS, not significant. B, HGF production by tumor tissues. Tumors were harvested on days 4 and 8 and lysed, and HGFs in the lysates were assayed by ELISA. All samples were assayed in triplicate. C, fibroblast-derived HGF induced TAE684 resistance via the Akt signal pathway *in vivo*. Tumors were harvested 2 hours after treatment on day 7 and lysed, and the lysates were analyzed by immunoblotting with the indicated antibodies, as described in Materials and Methods. The results shown are representative of 2 independent experiments.

Discussion

We have shown here that endothelial cells and fibroblasts, both components of the tumor microenvironment, secreted EGFR ligands and HGF, respectively, causing resistance to the ALK inhibitors crizotinib and/or TAE684 by activating bypass survival signals.

Of the EGFR ligands, EGF and TGF-α bind predominantly to EGFR, whereas HB-EGF binds to EGFR and ErbB4 (17). H2228 cells expressed both EGFR and ErbB4. Our results suggested that the bypass survival signal induced by EGFR ligands is mediated mainly by EGFR, as EGFR ligands markedly activated the phosphorylation of EGFR, not ErbB4. Moreover, knockdown of EGFR abrogated resistance caused by all EGFR ligands tested. EGFR ligand–triggered resistance was canceled by erlotinib or cetuximab, an anti-EGFR Ab, drugs approved for the treatment of patients with NSCLC and colorectal cancer. In addition, AP26113, an inhibitor of both ALK and EGFR, has been reported active against *EML4-ALK* lung cancer cells with amplified *ALK* and secondary mutations (7). Therefore, clinical trials are warranted to evaluate the efficacy and feasibility of combinations of an ALK inhibitor and these EGFR inhibitors to overcome ALK inhibitor resistance.

HGF, the sole ligand of Met (29), is important in EGFR-TKI resistance in *EGFR*-mutant lung cancer. HGF derived from cancer cells or stromal fibroblasts activated Met phosphorylation and stimulated the downstream Akt and Erk1/2 pathways (21, 22, 30) using Gab1, an adaptor protein for Met (31), triggering resistance to both reversible and irreversible EGFR-TKIs. In our Japanese cohort study of patients with *EGFR*-mutant lung cancer, high HGF expression was detected in 61% of tumors with acquired resistance and in 29% of tumors with intrinsic resistance to EGFR-TKIs, suggesting the rationale of targeting HGF to overcome EGFR-TKI resistance (32). We also found that HGF triggered TAE684 resistance by activating Met and stimulating downstream Akt and Erk1/2 pathways using the adaptor protein Gab1. Because many anti-HGF Abs and Met-TKIs are being evaluated in clinical trials, HGF-triggered resistance to selective ALK inhibitors may be controlled by their combinations in the near future.

EGFR and Met have been shown to interact with each other and to mediate redundant signaling in lung cancer cells (33). In *EGFR*-mutant lung cancer cells, *Met* amplification causes EGFR-TKI resistance by triggering bypass survival signals using ErbB3, an adaptor protein (34). Met activation by HGF also triggers resistance to EGFR-TKIs that use Gab1 as an adaptor. In *EML4-ALK* lung cancer cells, both novel ALK second mutations and autocrine EGFR activation causes resistance to ALK inhibitors (11). We found that paracrine HGF and EGFR ligands could trigger ALK inhibitor resistance. Taken together, these findings suggest that signaling by EGFR and Met is crucial for the survival of lung cancer cells with *EGFR* mutations and *EML4-ALK* translocations under inhibition of these driver oncogenes.

We found that resistance to TAE684 was induced by both EGFR ligands and HGF, whereas crizotinib resistance was induced by EGFR ligands alone, a finding that may be due to the dual activities of crizotinib on ALK and

Published OnlineFirst May 2, 2012; DOI:10.1158/1078-0432.CCR-11-2972

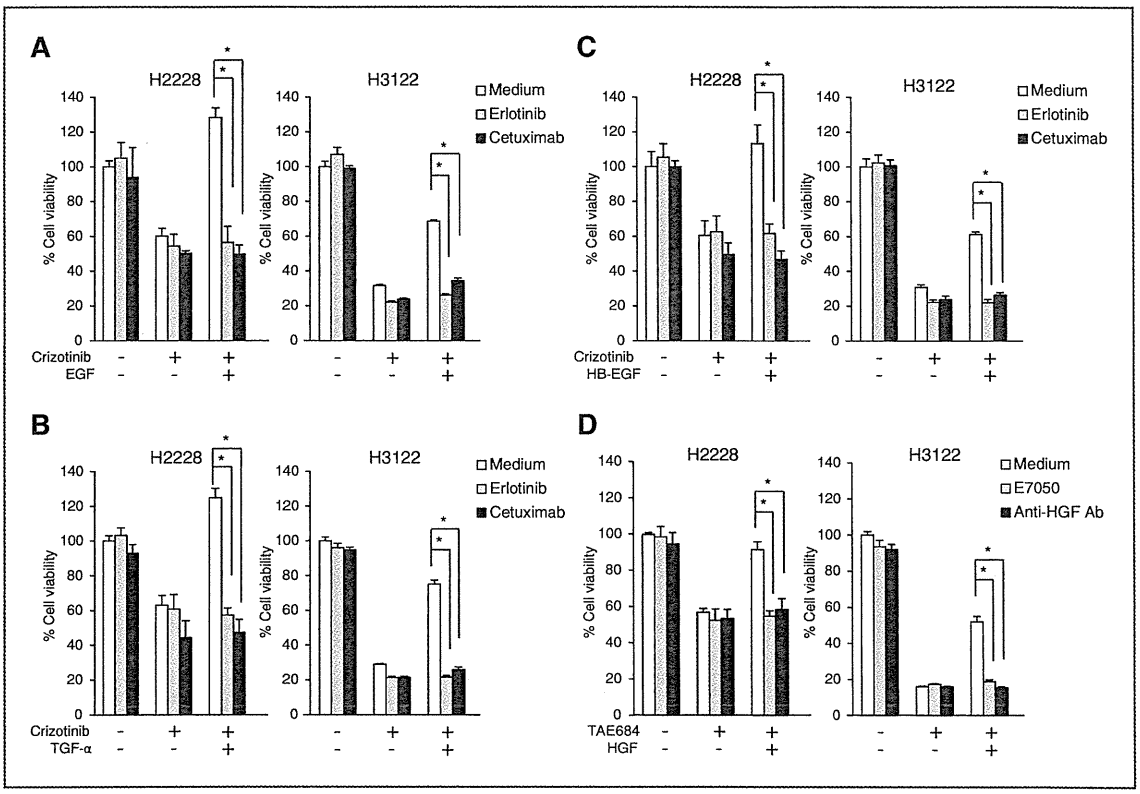

Figure 6. Ligand-triggered resistance to ALK inhibitors is abrogated by inhibitors of both HGF-Met and EGFR. A–C, the EGFR inhibitors erlotinib and cetuximab abrogated EGFR ligand-induced crizotinib resistance in EML4-ALK lung cancer cells. H2228 and H3122 cells were treated for 72 hours with or without crizotinib (100 nmol/L) and/or EGF (100 ng/mL), TGF-α (100 ng/mL), or HB-EGF (10 ng/mL) in the presence or absence of erlotinib (1 μmol/L) or cetuximab (2 μg/mL). Cell growth was determined by MTT assays. *, $P < 0.01$ (one-way ANOVA). Each experiment included triplicate determinations, and each experiment was repeated at least 3 times independently. D, Met-TKI E7050 or Anti-HGF antibody abrogated HGF-induced TAE684 resistance in EML4-ALK lung cancer cells. H2228 and H3122 cells were treated for 72 hours with or without TAE684 (100 nmol/L) and/or HGF (50 ng/mL) in the presence or absence of E7050 (1 μmol/L) or anti-HGF–neutralizing antibody (2 μg/mL). Cell growth was determined by MTT assays. *, $P < 0.01$ (one-way ANOVA). Each experiment included triplicate determinations, and each experiment was repeated at least 3 times independently.

Met (5). Selective ALK inhibitors are expected to be effective against *EML4-ALK* lung cancer cells, even after acquiring *ALK* amplification and *ALK* second mutations and becoming refractory to crizotinib (7, 35). Our findings, however, suggest that HGF-triggered resistance may be directed against selective ALK inhibitors, not crizotinib. Future clinical trials with selective ALK inhibitors may reveal the class of ALK inhibitors that is more beneficial for *EMK4-ALK* lung cancer patients.

EML4-ALK- and *EGFR*-mutant lung cancers show dramatic responses to ALK inhibitors and EGFR-TKIs, respectively (5, 36, 37). Complete responses, however, are rarely achieved, despite these cells express the target (EML4-ALK or mutant EGFR) of the drug. Low expression of BIM, a proapoptotic molecule, may explain, at least in part, the variations in sensitivity of *EGFR*-mutant lung cancer to EGFR-TKIs (38). This heterogeneous sensitivity may also be explained by HGF, as HGF is expressed more or less equally in *EGFR*-mutant lung tumors sensitive to EGFR-TKIs (32). Therefore, EGFR ligands in EML4-ALK lung tumors may be involved in their heterogeneous response to crizotinib. It is also curious whether ligand-triggered resistance is an independent mechanism or one that provided partial resistance when combined with another mechanism. Because crizotinib is expected to be approved in Japan to treat EML4-ALK lung cancer in 2012, we are planning a study to assess this possibility in clinical specimens.

In conclusion, we found that receptor ligands, such as EGFR ligands and HGF, could cause resistance to the ALK inhibitors crizotinib and/or TAE684 by activating bypass survival signals. These ligands and growth factors may be produced by host stromal cells, which constitute the cancer microenvironment. Paracrine HGF from stromal fibroblasts may also trigger resistance to EGFR-TKIs in EGFR-mutant lung cancer cells by activating bypass signals (22). Collectively, these observations suggest that paracrine receptor activation by the microenvironment

Published OnlineFirst May 2, 2012; DOI:10.1158/1078-0432.CCR-11-2972

may be an important mechanism inducing resistance to molecular targeted drugs in oncogene-activated lung cancer cells. These findings suggest that targeting of receptor ligands may result in more successful therapy in lung cancer.

Disclosure of Potential Conflicts of Interest

S. Yano received honoraria from Chugai Pharma and AstraZeneca and research fundings from Chugai Pharma and Eisai co., ltd. H. Mano received honoraria from Pfizer Inc., and T. Nakagawa and T. Uenaka are employees of Eisai co., ltd. The other authors disclosed no potential conflicts of interest.

Authors' Contributions

Conception and design: T. Yamada, S. Takeuchi, S. Yano
Development of methodology: T. Yamada
Analysis and interpretation of data (e.g., statistical analysis, biostatistics, computational analysis): T. Yamada, H. Mano
Acquisition of data (provided animals, acquired and managed patients, provided facilities, etc.): K. Kita, T. Nakagawa, T. Uenaka
Writing, review, and/or revision of the manuscript: T. Yamada, S. Yano
Administrative, technical, or material support (i.e., reporting or organizing data, constructing databases): J. Nakade, S. Nanjo, T. Nakamura, K. Matsumoto, M. Soda, H. Mano, S. Yano
Study supervision: S. Yano

Acknowledgments

The authors thank Dr. Jeffrey A. Engelman (Massachusetts General Hospital Cancer Center) for providing the H3122 cells.

Grant Support

This study was supported by grants-in-aid for cancer research (T. Yamada, 23790902 and S. Yano, 21390256) and scientific research on innovative areas "Integrative Research on Cancer Microenvironment Network" (S. Yano, 22112010A01) from the Ministry of Education, Culture, Sports, Science, and Technology of Japan.

The costs of publication of this article were defrayed in part by the payment of page charges. This article must therefore be hereby marked *advertisement* in accordance with 18 U.S.C. Section 1734 solely to indicate this fact.

Received November 21, 2011; revised March 28, 2012; accepted April 17, 2012; published OnlineFirst May 2, 2012.

References

1. Soda M, Choi YL, Enomoto M, Takada S, Yamashita Y, Ishikawa S, et al. Identification of the transforming EML4-ALK fusion gene in non-small-cell lung cancer. *Nature* 2007;448:561–6.
2. Horn L, Pao W. EML4-ALK: honing in on a new target in non-small-cell lung cancer. J Clin Oncol 2009;27:4232–5.
3. Koivunen JP, Mermel C, Zejnullahu K, Murphy C, Lifshits E, Holmes AJ, et al. EML4-ALK fusion gene and efficacy of an ALK kinase inhibitor in lung cancer. Clin Cancer Res 2008;14:4275–83.
4. Choi YL, Takeuchi K, Soda M, Inamura K, Togashi Y, Hatano S, et al. Identification of novel isoforms of the EML4-ALK transforming gene in non-small cell lung cancer. Cancer Res 2008;68:4971–6.
5. Kwak EL, Bang YJ, Camidge DR, Shaw AT, Solomon B, Maki RG, et al. Anaplastic lymphoma kinase inhibition in non-small-cell lung cancer. N Engl J Med 2010;363:1693–703.
6. Choi YL, Soda M, Yamashita Y, Ueno T, Takashima J, Nakajima T, et al. ALK Lung Cancer Study Group. EML4-ALK mutations in lung cancer that confer resistance to ALK inhibitors. N Engl J Med 2010;363:1734–9.
7. Katayama R, Khan TM, Benes C, Lifshits E, Ebi H, Rivera VM, et al. Therapeutic strategies to overcome crizotinib resistance in non-small cell lung cancers harboring the fusion oncogene EML4-ALK. Proc Natl Acad Sci U S A 2011;108:7535–40.
8. Sasaki T, Okuda K, Zheng W, Butrynski J, Capelletti M, Wang L, et al. The neuroblastoma-associated F1174L ALK mutation causes resistance to an ALK kinase inhibitor in ALK-translocated cancers. Cancer Res 2010;70:10038–43.
9. Doebele RC, Pilling AB, Aisner DL, Kutateladze TG, Le AT, Weickhardt AJ, et al. Mechanisms of resistance to crizotinib in patients with ALK gene rearranged non-small cell lung cancer. Clin Cancer Res 2012;18:1472–82.
10. Katayama R, Shaw AT, Khan TM, Mino-Kenudson M, Solomon BJ, Halmos B, et al. Mechanisms of acquired crizotinib resistance in ALK-rearranged lung Cancers. Sci Transl Med 2012;4:120ra17.
11. Sasaki T, Koivunen J, Ogino A, Yanagita M, Nikiforow S, Zheng W, et al. A novel ALK secondary mutation and EGFR signaling cause resistance to ALK kinase inhibitors. Cancer Res 2011;71:6051–60.
12. Heuckmann JM, Hölzel M, Sos ML, Heynck S, Balke-Want H, Koker M, et al. ALK mutations conferring differential resistance to structurally diverse ALK inhibitors. Clin Cancer Res 2011;17:7394–401.
13. McAllister SS, Weinberg RA. Tumor-host interactions: a far-reaching relationship. J Clin Oncol 2010;28:4022–8.
14. Joyce JA, Pollard JW. Microenvironmental regulation of metastasis. Nat Rev Cancer 2009;9:239–52.
15. Seruga B, Zhang H, Bernstein LJ, Tannock IF. Cytokines and their relationship to the symptoms and outcome of cancer. Nat Rev Cancer 2008;8:887–99.
16. Janku F, Stewart DJ, Kurzrock R. Targeted therapy in non-small-cell lung cancer–is it becoming a reality? Nat Rev Clin Oncol 2010;7:401–14.
17. Yasumoto K, Yamada T, Kawashima A, Wang W, Li Q, Donev IS, et al. The EGFR ligands amphiregulin and heparin-binding egf-like growth factor promote peritoneal carcinomatosis in CXCR4-expressing gastric cancer. Clin Cancer Res 2011;17:3619–30.
18. Matsumoto K, Nakamura T. Hepatocyte growth factor and the Met system as a mediator of tumor-stromal interactions. Int J Cancer 2006;119:477–83.
19. Masuya D, Huang C, Liu D, Nakashima T, Kameyama K, Haba R, et al. The tumour-stromal interaction between intratumoral c-Met and stromal hepatocyte growth factor associated with tumour growth and prognosis in non-small-cell lung cancer patients. Br J Cancer 2004;90:1555–62.
20. Meert AP, Martin B, Delmotte P, Berghmans T, Lafitte JJ, Mascaux C, et al. The role of EGF-R expression on patient survival in lung cancer: a systematic review with meta-analysis. Eur Respir J 2002;20:975–81.
21. Yamada T, Matsumoto K, Wang W, Li Q, Nishioka Y, Sekido Y, et al. Hepatocyte growth factor reduces susceptibility to an irreversible epidermal growth factor receptor inhibitor in EGFR-T790M mutant lung cancer. *Clin Cancer Res* 2010;16:174–83.
22. Wang W, Li Q, Yamada T, Matsumoto K, Matsumoto I, Oda M, et al. Crosstalk to stromal fibroblasts induces resistance of lung cancer to epidermal growth factor receptor tyrosine kinase inhibitors. Clin Cancer Res 2009;15:6630–8.
23. Soda M, Takada S, Takeuchi K, Choi YL, Enomoto M, Ueno T, et al. A mouse model for EML4-ALK-positive lung cancer. Proc Natl Acad Sci U S A 2008;105:19893–7.
24. Nakamura Y, Azuma M, Okano Y, Sano T, Takahashi T, Ohmoto Y, et al. Upregulatory effects of interleukin-4 and interleukin-13 but not interleukin-10 on granulocyte/macrophage colony-stimulating factor production by human bronchial epithelial cells. Am J Respir Cell Mol Biol 1996;15:680–7.
25. Koren HS, Anderson SJ, Larrick JW. *In vitro* activation of a human macrophage-like cell line. Nature 1979;279:328–31.
26. Kuniyasu H, Yano S, Sasaki T, Sasahira T, Sone S, Ohmori H. Colon cancer cell-derived high mobility group 1/amphoterin induces growth inhibition and apoptosis in macrophages. Am J Pathol 2005;166:751–60.
27. Nakagawa T, Tohyama O, Yamaguchi A, Matsushima T, Takahashi K, Funasaka S, et al. E7050: a dual c-Met and VEGFR-2 tyrosine kinase

Cancer Science
The official journal of the Japanese Cancer Association

High-throughput resequencing of target-captured cDNA in cancer cells

Toshihide Ueno,[1,5] Yoshihiro Yamashita,[1,5] Manabu Soda,[1] Kazutaka Fukumura,[2] Mizuo Ando,[2] Azusa Yamato,[1] Masahito Kawazu,[2] Young Lim Choi[1,2] and Hiroyuki Mano[1,2,3,4]

[1]Division of Functional Genomics, Jichi Medical University, Tochigi; [2]Department of Medical Genomics, Graduate School of Medicine, University of Tokyo, Tokyo; [3]CREST Japan Science and Technology Agency, Saitama, Japan

(Received May 30, 2011/Revised September 7, 2011/Accepted September 14, 2011/Accepted manuscript online September 20, 2011/Article first published online October 13, 2011)

The recent advent of whole exon (exome)-capture technology, coupled with second-generation sequencers, has made it possible to readily detect genomic alterations that affect encoded proteins in cancer cells. Such target resequencing of the cancer genome, however, fails to detect most clinically-relevant gene fusions, given that such oncogenic fusion genes are often generated through intron-to-intron ligation. To develop a resequencing platform that simultaneously captures point mutations, insertions–deletions (indels), and gene fusions in the cancer genome, we chose cDNA as the input for target capture and extensive resequencing, and we describe the versatility of such a cDNA-capture system. As a test case, we constructed a custom target-capture system for 913 cancer-related genes, and we purified cDNA fragments for the target gene set from five cell lines of CML. Our target gene set included Abelson murine leukemia viral oncogene homolog 1 (*ABL1*), but it did not include breakpoint cluster region (*BCR*); however, the sequence output faithfully detected reads spanning the fusion points of these two genes in all cell lines, confirming the ability of cDNA capture to detect gene fusions. Furthermore, computational analysis of the sequence dataset successfully identified non-synonymous mutations and indels, including those of tumor protein p53 (*TP53*). Our data might thus support the feasibility of a cDNA-capture system coupled with massively parallel sequencing as a simple platform for the detection of a variety of anomalies in protein-coding genes among hundreds of cancer specimens. (*Cancer Sci* 2012; 103: 131–135)

Cancer is thought to result from various alterations of the genome, including point mutations, insertions–deletions (indels), and genomic rearrangements.[1] Whereas comprehensive sequencing of the cancer genome, or "cancer genome resequencing", is a promising approach to the identification of such anomalies, and to provide a basis for the development of effective treatment strategies for cancer, determination of the nucleotide sequence of the entire human genome with conventional Sanger sequencers remains a highly demanding task. However, the recent advent of massively parallel sequencing systems, or second-generation sequencers, has rendered such projects manageable in private laboratories[2] and triggered the formation of large-scale consortia, such as The Cancer Genome Atlas and International Cancer Genome Consortium,[3] to undertake cancer genome resequencing for hundreds of specimens. Cancer genome resequencing with massively parallel sequencers has already provided a wealth of information on genome-wide mutation status for melanoma,[4] acute myeloid leukemia,[5] hepatocellular carcinoma,[6] and other cancers.

Even with the current massively parallel sequencers, however, the determination and compilation of the full genome sequence for a given sample might still take almost 1 month. Comparison of the cancer genome among many specimens thus remains time-consuming and labor intensive. Anomalies in protein-coding genes likely play a major role in carcinogenesis. Given that exonic regions occupy only ~1.3% of the human genome, sequencing such targeted regions would be expected to markedly facilitate the discovery of proteins that are activated or inactivated specifically in cancer cells. Indeed, target-capture strategies, coupled with massively parallel sequencers, have revealed important genetic changes in cancer,[7] as well as in hereditary disorders.[8,9]

One important drawback of such target-capture approaches, however, is their inability to detect gene fusions. Most cancer-associated gene fusion events occur within introns (resulting in exon-to-exon ligation in the corresponding mRNA), and exon capture does not reveal breakage and ligation of intronic regions. Recurrent gene fusions were once thought to be rare in epithelial tumors compared with hematologic malignancies and sarcomas;[10] however, our recent discovery of the echinoderm microtubule associated protein like-4 (EML4)-anaplastic lymphoma kinase (ALK) fusion gene in lung cancer and the discovery by others of rearrangements in loci for the v-ets avian erythroblastosis virus E26 oncogene homolog (ETS) family of transcription factors in prostate cancer have led to a revision of this notion.[11,12] It would thus be desirable to develop a resequencing platform that is able to capture, within a reasonable timeframe, all gene fusions, point mutations, and indels in the cancer genome. In pursuit of this goal, we have now examined the efficacy of high-throughput sequencing of captured cDNA for the identification of such cancer genome anomalies.

Materials and Methods

Cell lines. Cell lines established from the blast crisis stage of CML, including MEG-01s, KCL-22-SR, K562, NCO2, and KU812,[13,14] were obtained from the Japanese Collection of Research Bioresources (Osaka, Japan) and were maintained in RPMI-1640 medium (Invitrogen, Carlsbad, CA, USA) supplemented with 10% FBS (Invitrogen). Total RNA was isolated from each cell line with the use of an RNeasy mini kit (Qiagen, Valencia, CA, USA) and was subjected to cDNA synthesis with an oligo(dT) primer.

Gene expression profiling. The cDNA prepared from total poly(A)-RNA of KCL-22-SR cells was subjected to hybridization with the HGU95Av2 microarray (Affymetrix, Santa Clara, CA, USA), as described previously.[15] The expression intensity of each test gene on the array was normalized by the 50th percentile value.

cDNA-capture methods. RNA probes of 120 bases were designed to cover (with a 60-base overlap) cDNA of 913 human protein-coding genes (Table S1), and were synthesized by Agilent Technologies (Santa Clara, CA, USA). During the design of the probes, the Repeat Masker dataset (http://www.repeatmasker.org) was used to remove probes corresponding to

[4]To whom correspondence should be addressed. E-mail: hmano@jichi.ac.jp
[5]These authors contributed equally to this work.

doi: 10.1111/j.1349-7006.2011.02105.x

repetitive sequences in the human genome. Hybridization of DNA fragments to the RNA probes was performed according to the protocols recommended for the SureSelect Target Enrichment system (Agilent). We also used the SureSelect Human X Chromosome Demo kit (Agilent) to examine purification efficiency. Purified DNA fragments were then subjected to sequencing with a Genome Analyzer IIx (GAIIx; Illumina, San Diego, CA, USA) for 76 bases from both ends by the paired-end sequencing system.

Computational pipeline. Raw read data were quality filtered on the basis of the presence of the Illumina adaptor sequences and a *Q*-value of ≥20. The resulting read sequences were then subjected to an in-house computational pipeline to identify various mutations (Fig. S1). In brief, read sequences were matched with the Bowtie algorithm[16] to the cDNA sequences of the 913 genes used to construct our custom-made SureSelect system. The matched reads were then examined for the presence of non-synonymous mutations and single nucleotide polymorphisms (SNP) deposited in dbSNP (build 132, http://www.ncbi.nlm.nih.gov/projects/SNP/index.html). The remaining reads were further matched to the cDNA sequences with Burrows-Wheeler Aligner (BWA) and Basic Local Alignment Search Tool (BLAST) algorithms to search for indels and multiple mutations.[17,18] Candidates for non-synonymous mutations were identified only when ≥20% of reads correspond to the mutations at positions with ≥50 coverage.

For the selection of reads corresponding to possible fusion cDNA, nucleotide sequences of 20 bp were obtained from both ends of each read and were separately matched to RefSeq mRNA (http://www.ncbi.nlm.nih.gov), KnownGeneMrna,[19] and the human genome sequence (GRCh37, http://www.ncbi.nlm.nih.gov/projects/genome/assembly/grc/human/data/?build=37). Reads were considered to be derived from fusion genes if the ends of a given read matched to different genes within the 913-gene group, or one end matched to a single gene within the 913-gene group and the other end matched to a sequence in RefSeq, KnownGeneMrna, or the human genome sequence that did not correspond to the 913 genes. Candidates for fusion genes were identified only when four or more reads were mapped to possible fusion points.

RT–PCR. To confirm the presence of an alternatively-spliced mixed-lineage leukemia (*MLL*) mRNA, we subjected oligo(dT)-primed cDNA of KU812 cells to PCR with the combination of the F-1 primer (5′-ACCTCGTGGGAGACCTAGAAGTGG-3′) and the R primer (5′-AGTCATTGGAAGCTTGTCTGCCTG-3′), or with the combination of the F-2 primer (5′-CCTGTGGGTA-GGGTTTCCAAAGAG-3′) and the R primer.

Results

Efficiency of cDNA-capture sequencing. Paired-end sequencing of target-captured cDNA was briefly described in a previous study;[20] however, how the efficiency of target purification with cDNA compares with that with genomic DNA remains unclear. We therefore attempted to optimize the conditions for cDNA purification with the SureSelect system. Oligo(dT)-primed cDNA of KCL-22-SR cells were fragmented to a mean size of 500 or 200 bp and then subjected to purification with the use of the SureSelect Human X Chromosome Demo kit, which is designed to capture genomic sequences derived from the human X chromosome. Genomic DNA of KCL-22-SR cells was similarly processed and hybridized with the X Chromosome Demo kit. The purified fragments at either 4 or 8 pM were then sequenced by the GAIIx system.

The X chromosome-mapped cDNA reads occupied 62.1%, 81.6%, 62.4%, and 82.2% of quality filter-passed reads for the experiments with 4 pM of 500-bp fragments, 4 pM of 200-bp fragments, 8 pM of 500-bp fragments, and 8 pM of 200-bp fragments, respectively (Fig. 1). Thus, these results suggested that the shorter cDNA fragments were captured more efficiently than the longer ones. Furthermore, the purification efficiency for genomic DNA fragments was not higher than that for cDNA, irrespective of DNA concentration and fragmentation size (Fig. 1), supporting the feasibility of cDNA-capture approaches.

The ability to detect breakpoint cluster region (*BCR*)-Abelson murine leukemia viral oncogene homolog 1 (*ABL1*) fusion reads was reduced for the cDNA sheared to ~200 bp compared with that for those of ~500 bp (see below). The former cDNA detected 83.7% or 76% of the fusion reads detected by the latter cDNA at input concentrations of 4 and 8 pM, respectively. This result is in line with our computational bootstrap trial (n = 10 000) showing that the number of randomly-fragmented, 200-bp reads encompassing the *BCR–ABL1* fusion point is ~2.5 times higher than that of 500-bp reads (data not shown). However, given that the total number of high-quality reads was much higher in the data for the 200-bp cDNA than in those for the 500-bp cDNA (Fig. 1), we chose to use 8 pM of cDNA with a mean size of 200 bp for further experiments.

Custom cDNA-capture system. We also tested whether extensive sequencing of cDNA generated from total poly(A)-RNA (unselected cDNA) might serve to identify gene fusions, point mutations, and indels. For this purpose, unselected cDNA were prepared from KCL22-SR cells, and subjected to GAIIx sequencing, yielding 34.1 million reads, which mapped to 36 128 RefSeq entries (data not shown). The distribution of read number per transcript in the data is shown in Figure 2a. Among the 36 128 entries, only 200 (0.55%) accounted for ~20% of total reads, and 4.55% accounted for ~50% of reads. Thus, as expected, resequencing data for unselected cDNA consist mostly of reads corresponding to a limited number of highly-abundant transcripts.

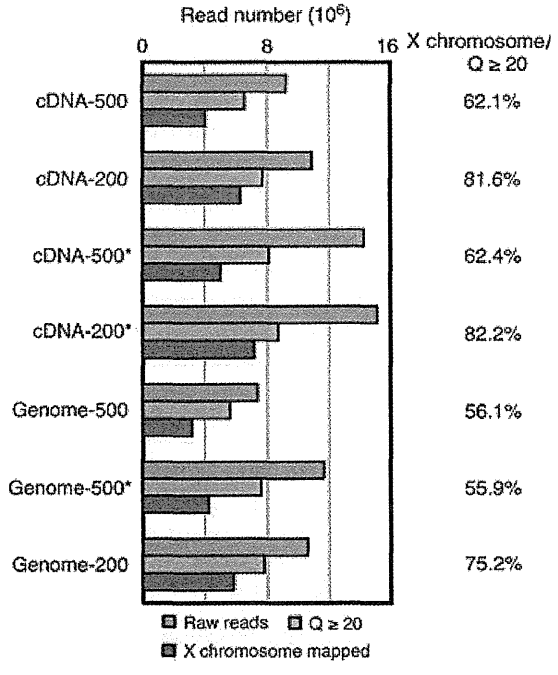

Fig. 1. Comparison of capture efficiency between cDNA and genomic DNA. Genomic DNA or cDNA of KCL-22-SR cells was fragmented to a mean size of 200 or 500 bp, and then subjected to purification with the SureSelect Human X Chromosome Demo kit, followed by GAIIx sequencing at a concentration of 4 or 8 pM (the latter indicated by an asterisk). Numbers of raw reads, reads with a *Q*-value of ≥20 ($Q \geq 20$), and reads mapped to the human X chromosome are shown for each experiment. Percentage of X chromosome-mapped reads among the reads with a *Q*-value of ≥20 is shown on the right.

doi: 10.1111/j.1349-7006.2011.02105.x

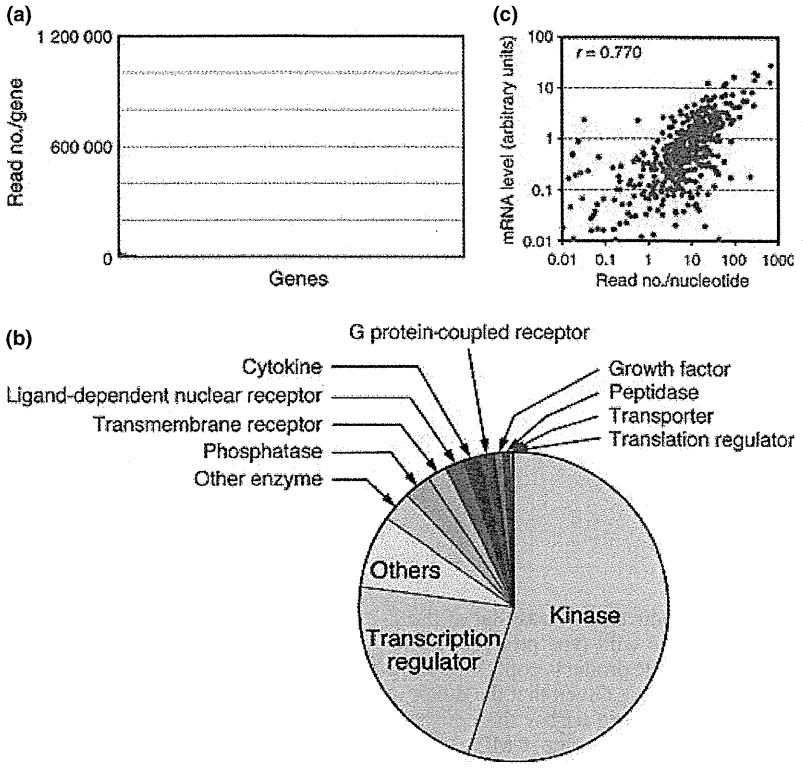

Fig. 2. Capture of a selected set of cDNA. (a) Read number for each gene was calculated from the sequencing data for the unselected cDNA of KCL-22-SR cells. Genes were sorted according to their read number. A small number of genes accounted for most of the sequence reads. (b) Functional annotation for the encoded proteins of our target cDNA (n = 913). (c) Read number per nucleotide for each captured cDNA in KCL-22-SR cells is compared with the expression intensity (arbitrary units) of the same cDNA examined with an HGU95Av2 microarray. Pearson's correlation coefficient (r) for the comparison is also demonstrated.

We therefore attempted to construct a custom SureSelect system to capture cDNA for cancer-related genes. For this purpose, we selected 913 genes that yielded 56 892 hybridization probes corresponding to ~3.77 Mbp of total capture capacity. The target genes encoded human protein kinases (all members in the human genome), transcription regulators, phosphatases, and other proteins (Fig. 2b; Table S1).

To compare the information provided by the sequence data from unselected and captured cDNA, we purified target cDNA from KCL-22-SR cells with the use of our custom SureSelect system, and determined their nucleotide sequences with GAIIx. A comparable amount of filter-passed reads (39.2 million) to that of unselected cDNA were thus obtained. We found that 88% of the captured cDNA were mapped to the target genes in our SureSelect system, while only 6.6% of the unselected cDNA were mapped to the 913 targets (data not shown). The read number obtained for each gene in the captured cDNA dataset is shown in Figure S2, with the distribution being markedly different from that obtained by sequencing of the unselected cDNA (Fig. 2a). As expected, the read number per nucleotide in each cDNA for the captured dataset was highly correlated to the expression intensity of the same gene quantified with the HGU95Av2 GeneChip expression array (Pearson's correlation coefficient = 0.770, $P < 2.2 \times 10^{-16}$) (Fig. 2c).

We further isolated target cDNA from other CML cell lines, including K562, KU812, MEG-01s, and NCO2, and the purified cDNA fragments were subjected to GAIIx sequencing. As in the case for KCL-22-SR, 86–88% of the obtained reads were successfully mapped to the target cDNA in each cell line (Table S2).

Screening of fusion cDNA. Our target set of 913 genes did not include *BCR*, but it did contain *ABL1*. Thus, if we were able to isolate sequence reads encompassing the fusion point of *BCR–ABL1*, cDNA-capture approaches for a given gene set would likely be able to detect gene fusions to unknown partners. In fact, we detected 45 sequence reads for KCL-22-SR cells that covered the *BCR–ABL1* fusion point (Fig. 3a). Likewise, the sequence datasets for K562, KU812, MEG-01s, and NCO2 cells contained 53, 8, 11, and 10 such fusion reads, respectively (data not shown). Furthermore, our sequence data faithfully recapitulated two variants of *BCR–ABL1* cDNA in these cell lines; a fusion variant between exon 13 of *BCR* and exon 2 of *ABL1* was detected in KCL-22-SR, MEG-01s, and NCO2 cells, whereas a fusion variant between exon 14 of *BCR* and exon 2 of *ABL1* was detected in K562 and KU812 cells.[14]

In addition to *BCR–ABL1*, we identified 72 independent candidates for fusion cDNA (including fusions to non-coding RNA) from the CML cell lines. Surprisingly, however, the screening of fusion genes among the unselected cDNA of KCL-22-SR with our rather non-stringent threshold (≥4 reads mapped to a candidate fusion point) failed to isolate *BCR–ABL1* cDNA. We could not even detect any fusion candidates (involving one of our target genes in either or both ends of fusion events) from this dataset, while a total of nine candidates (including *BCR–ABL1*) were isolated from the captured cDNA of the same cell line.

Our Bowtie mapping of both ends of each read to human mRNA or genome databases (Fig. S1) resulted in the detection of not only *BCR–ABL1* fusions, but also a large number of alternatively-spliced messages. From the captured cDNA of KCL-22-SR, for instance, we could detect 79 alternatively-spliced transcripts for 72 independent genes (data not shown). In contrast, from the unselected cDNA of the same cell line, only three independent, alternatively-spliced transcripts were identified among three genes within the 913 targets.

One such example of alternatively-spliced message was *MLL* (ensemble accession no.: ENST00000389506) in KU812, MEG-01s, and K562 cells. In addition to a set of reads that completely matched exon 3 of *MLL*, we obtained reads that lacked an internal 2193-bp sequence in exon 3 (Fig. 3b). Such in-frame truncation would be expected to generate an MLL protein lacking amino acids 276–1006 of the wild-type protein. To confirm the presence of such transcripts, we performed RT–PCR analysis with total RNA from KU812 cells, and PCR primers designed as in Figure 3b. The combination of the F-1 and R primers would be expected to yield both the wild-type (2536 bp) and truncated

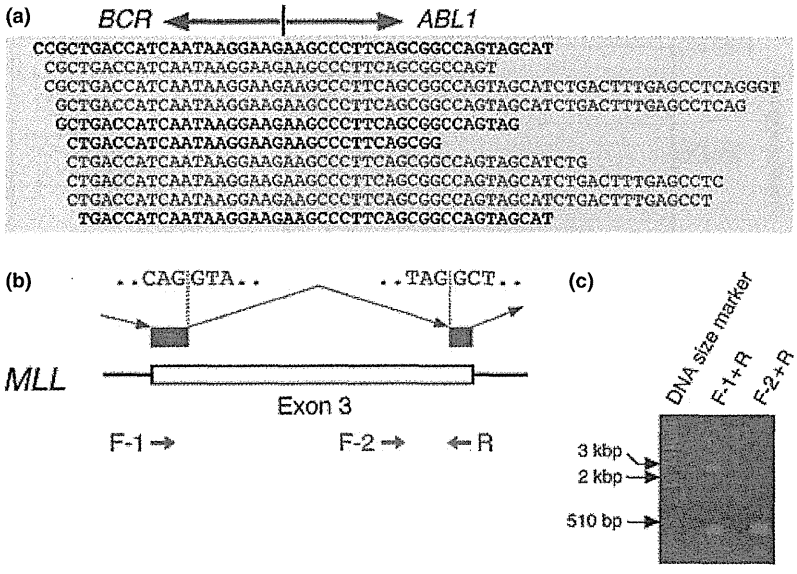

Fig. 3. Detection of gene fusions and alternative mRNA splicing in CML cells. (a) Our computational pipeline yielded 45 reads for KCL-22-SR cells that encompassed the fusion point of breakpoint cluster region (*BCR*)-Abelson murine leukemia viral oncogene homolog 1 (*ABL1*) cDNA, some of which are shown aligned. Reads in the sense or antisense strand are designated in black and blue letters, respectively, and the *BCR* and *ABL1* portions of the sequences are shaded differentially. (b) Some of the reads that mapped to exon 3 of mixed-lineage leukemia (*MLL*) skipped a 2193-bp region within this exon. Nucleotide sequences of the cryptic splicing sites are shown, as are the positions of PCR primers used to confirm the alternative splicing. (c) Gel electrophoresis of the RT–PCR products obtained with total RNA isolated from KU812 cells and with either the F-1 and R primer pair or the F-2 and R primer pair. A 1-kb ladder of DNA size markers was also included.

(343 bp) products, whereas that of the F-2 and R primers would yield only the wild-type product of 339 bp. Gel electrophoresis of the RT–PCR products confirmed the presence of the truncated mRNA (Fig. 3c). Given that the donor and acceptor sites for this alternative splicing harbor the consensus sequences for mRNA splicing (Fig. 3b), some CML cells likely make use of such cryptic splicing sites after *MLL* transcription.

Other variants. From the captured cDNA for KCL-22-SR, NCO2, MEG-01s, K562, and KU812 cells; we detected 156, 18, 28, 23, and 21 non-synonymous mutations among the 913 target genes, respectively. An analysis of the unselected cDNA from KCL-22-SR, however, identified only 19 mutations within the target genes, 16 of which were discovered in the captured cDNA as well. Comparison of the read sequences from the unselected KCL-22-SR cDNA to all RefSeq exonic sequences discovered a total of 597 non-synonymous mutations.

Furthermore, 19, eight, four, 11, and two indels were detected with the captured cDNA of KCL-22-SR, NCO2, MEG-01s, K562, and KU812, respectively. Most of the detected indels were only 1 bp in length, whereas the others were either 2 or 3 bp (Fig. S3). Detailed analysis of these nucleotide changes will be described elsewhere (Toshihide Ueno and Yoshihiro Yamashita, personal communication).

One of the most frequent genetic changes in the blast crisis of CML is point mutation or loss (or both) of *TP53*.[21] Indeed, our sequence data for this gene revealed non-synonymous point mutations in NCO2 and KU812 cells, a 1-bp insertion in K562 cells, a 1-bp deletion in KCL-22-SR cells, and a 3-bp deletion in MEG-01s cells (Fig. 4; Fig. S4; Table S3), all of which were confirmed by Sanger sequencing (data not shown). In NCO2 cells, for instance, 100% of *TP53* reads harbored a G-to-C substitution at nucleotide position 993 of *TP53* mRNA (GenBank accession no.: NM_000546), resulting in a glycine-to-arginine amino acid change (Fig. 4a). The data were also indicative of loss of heterozygosity for *TP53* in NCO2 cells. Similarly, 75% or 78% of *TP53* reads contained a C insertion or a CAC deletion in K562 (Fig. 4b) or MEG-01s (Fig. S4) cells, respectively.

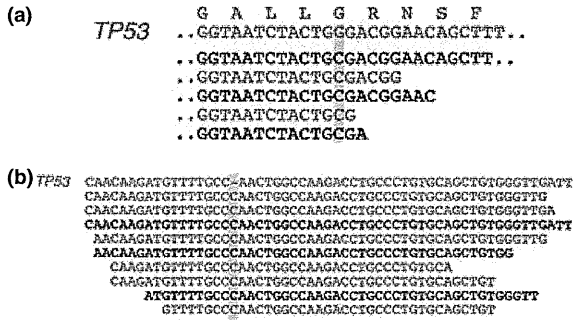

Fig. 4. Anomalies in *TP53* in CML cell lines. (a) Read sequences for NCO2 cells are shown aligned with the reference nucleotide and predicted amino acid sequences (red letters) for *TP53*, revealing a G-to-C substitution in all the reads. Sense or antisense strands are denoted in black and blue letters, respectively. (b) Alignment of the read sequences for K562 cells with the cDNA sequence of *TP53* as in (a), revealing a C insertion.

Discussion

We have shown that a cDNA-capture system, coupled with massively parallel sequencing, is a feasible and relatively simple approach to the simultaneous detection of point mutations, indels, and gene fusions in target cDNA. There are, however, both advantages and disadvantages of this technique compared with the conventional exon-capture system for genomic DNA.

The ability to detect gene fusions, in addition to other mutations with a single sequencing reaction, is one of the most important benefits of the cDNA-capture approach. Furthermore, the efficiency of exon capture with genomic DNA is dependent on the sequence context of each exon. The mean exon size for the human genome is only <200 bp, and the efficiency of exon purification is markedly affected by GC content and sequence complexity.[22] In contrast, even exons with a high GC content might be well isolated by the cDNA-capture system if adjacent exons have a normal GC content and are efficiently targeted by hybridization probes.

Levin *et al.*[20] conducted deep sequencing of captured cDNA for K562 cells, and identified five candidates for fusion genes in addition to *BCR–ABL1*. However, we could not detect any of the five candidates through our analysis with K562, probably because our 913 target genes did not contain those involved in the gene fusions in their report, other than nascent polypeptide-associated complex alpha subunit (*NACA*). While Levin *et al.* discovered primase, DNA, polypeptide 1 (*PRIM1*)–*NACA* fusion transcripts, the low expression level of *PRIM1–NACA* in K562 (only 2.5% of that of *BCR–ABL1* in their dataset)[20] might account for the failure in our analysis.

doi: 10.1111/j.1349-7006.2011.02105.x

However, for experiments based on capture of genomic DNA, sequencing a paired normal specimen allows the efficient subtraction of rare SNP not present in the current databases from the dataset of cancer tissue. This is not always the case, however, for the cDNA-capture approach, given that gene expression profiles differ markedly among samples (even among those obtained from the same individual). Genes with sequence alterations in the cancer specimen might not be expressed in a given normal specimen, and it is not possible to readily determine whether such alterations are germ-line polymorphisms, while algorithms to predict the effect on protein functions for a given amino acid change are currently available[23] and synonymous-to-non-synonymous ratio of nucleotide alterations for a given gene/dataset might provide clues as to how such changes are selected in tumor cells.[24]

In addition, the cDNA-capture system cannot obtain a sufficient number of reads for genes expressed at a low level, and the overall sensitivity of cDNA capture is dependent on the total read number provided by sequencers. We are able to run only two samples per flow cell of the GAIIx system, whereas up to eight samples can be run in a single flow cell for whole exome sequencing of human genomic DNA.

Despite such limitations, our study shows that cDNA capture is an efficient process, and extensive sequencing of such purified cDNA is a straightforward approach to interrogate the target cDNA for various genetic changes in a single platform. Large-scale resequencing of hundreds of cancer specimens might thus become within the scope of private laboratories with the adoption of the cDNA-capture approach.

Acknowledgments

This study was supported in part by grants for Research on Human Genome Tailor-Made and for Third-Term Comprehensive Control Research for Cancer from the Ministry of Health, Labor, and Welfare of Japan; Grants-in-Aid for Scientific Research (B) and for Young Scientists (A) from the Ministry of Education, Culture, Sports, Science, and Technology of Japan; and by grants from the Japan Society for the Promotion of Science, Takeda Science Foundation, the Naito Foundation, Sankyo Foundation of Life Science, The Sagawa Foundation for Promotion of Cancer Research, the Yasuda Medical Foundation, the Mitsubishi Foundation, and Kobayashi Foundation for Cancer Research.

Disclosure Statement

K. Fukumura, M. Ando, M. Kawazu, Y.L. Choi and H. Mano belong to the Department of Medical Genomics, Graduate School of Medicine, University of Tokyo, which receives research funding from Illumina Inc.

References

1 Stratton MR, Campbell PJ, Futreal PA. The cancer genome. *Nature* 2009; **458**: 719–24.
2 Mardis ER. A decade's perspective on DNA sequencing technology. *Nature* 2011; **470**: 198–203.
3 Ledford H. Big science: the cancer genome challenge. *Nature* 2010; **464**: 972–4.
4 Pleasance ED, Cheetham RK, Stephens PJ *et al.* A comprehensive catalogue of somatic mutations from a human cancer genome. *Nature* 2010; **463**: 191–6.
5 Ley TJ, Mardis ER, Ding L *et al.* DNA sequencing of a cytogenetically normal acute myeloid leukaemia genome. *Nature* 2008; **456**: 66–72.
6 Totoki Y, Tatsuno K, Yamamoto S *et al.* High-resolution characterization of a hepatocellular carcinoma genome. *Nat Genet* 2011; **43**: 464–9.
7 Wei X, Walia V, Lin JC *et al.* Exome sequencing identifies GRIN2A as frequently mutated in melanoma. *Nat Genet* 2011; **43**: 442–6.
8 Otto EA, Hurd TW, Airik R *et al.* Candidate exome capture identifies mutation of SDCCAG8 as the cause of a retinal-renal ciliopathy. *Nat Genet* 2010; **42**: 840–50.
9 Bilguvar K, Ozturk AK, Louvi A *et al.* Whole-exome sequencing identifies recessive WDR62 mutations in severe brain malformations. *Nature* 2010; **467**: 207–10.
10 Mitelman F. Recurrent chromosome aberrations in cancer. *Mutat Res* 2000; **462**: 247–53.
11 Soda M, Choi YL, Enomoto M *et al.* Identification of the transforming *EML4–ALK* fusion gene in non-small-cell lung cancer. *Nature* 2007; **448**: 561–6.
12 Tomlins SA, Rhodes DR, Perner S *et al.* Recurrent fusion of TMPRSS2 and ETS transcription factor genes in prostate cancer. *Science* 2005; **310**: 644–8.
13 Ohmine K, Nagai T, Tarumoto T *et al.* Analysis of gene expression profiles in an imatinib-resistant cell line, KCL22/SR. *Stem Cells* 2003; **21**: 315–21.
14 Drexler HG, MacLeod RA, Uphoff CC. Leukemia cell lines: *in vitro* models for the study of Philadelphia chromosome-positive leukemia. *Leuk Res* 1999; **23**: 207–15.
15 Choi YL, Tsukasaki K, O'Neill MC *et al.* A genomic analysis of adult T-cell leukemia. *Oncogene* 2007; **26**: 1245–55.
16 Langmead B, Trapnell C, Pop M, Salzberg SL. Ultrafast and memory-efficient alignment of short DNA sequences to the human genome. *Genome Biol* 2009; **10**: R25.
17 Altschul SF, Gish W, Miller W, Myers EW, Lipman DJ. Basic local alignment search tool. *J Mol Biol* 1990; **215**: 403–10.
18 Li H, Durbin R. Fast and accurate short read alignment with Burrows–Wheeler transform. *Bioinformatics* 2009; **25**: 1754–60.
19 Fujita PA, Rhead B, Zweig AS *et al.* The UCSC Genome Browser database: update 2011. *Nucleic Acids Res* 2011; **39**: D876–82.
20 Levin JZ, Berger MF, Adiconis X *et al.* Targeted next-generation sequencing of a cancer transcriptome enhances detection of sequence variants and novel fusion transcripts. *Genome Biol* 2009; **10**: R115.
21 Calabretta B, Perrotti D. The biology of CML blast crisis. *Blood* 2004; **103**: 4010–22.
22 Shen P, Wang W, Krishnakumar S *et al.* High-quality DNA sequence capture of 524 disease candidate genes. *Proc Natl Acad Sci USA* 2011; **108**: 6549–54.
23 Adzhubei IA, Schmidt S, Peshkin L *et al.* A method and server for predicting damaging missense mutations. *Nat Methods* 2010; **7**: 248–9.
24 Babenko VN, Basu MK, Kondrashov FA, Rogozin IB, Koonin EV. Signs of positive selection of somatic mutations in human cancers detected by EST sequence analysis. *BMC Cancer* 2006; **6**: 36.

Supporting Information

Additional Supporting Information may be found in the online version of this article:

Fig. S1. Algorithm of the computational pipeline.

Fig. S2. Read number distribution of all poly(A)-RNA data.

Fig. S3. Numbers of 1-, 2-, or 3-bp indels for the entire dataset.

Fig. S4. A CAG-deletion in the *TP53* message in MEG-01s cells.

Table S1. Gene list for the custom cDNA-capture system.

Table S2. Purification of the target cDNA in CML cell lines.

Table S3. TP53 mutation status in CML cell lines.

Please note: Wiley-Blackwell are not responsible for the content or functionality of any supporting materials supplied by the authors. Any queries (other than missing material) should be directed to the corresponding author for the article.

OPEN ACCESS Freely available online

PLoS one

KLC1-ALK: A Novel Fusion in Lung Cancer Identified Using a Formalin-Fixed Paraffin-Embedded Tissue Only

Yuki Togashi[1,2], Manabu Soda[3], Seiji Sakata[1], Emiko Sugawara[1,4], Satoko Hatano[1,2], Reimi Asaka[1,2], Takashi Nakajima[5], Hiroyuki Mano[3,6], Kengo Takeuchi[1,2]*

1 Pathology Project for Molecular Targets, The Cancer Institute, Japanese Foundation for Cancer Research, Tokyo, Japan, **2** Division of Pathology, The Cancer Institute, Japanese Foundation for Cancer Research, Tokyo, Japan, **3** Division of Functional Genomics, Jichi Medical University, Tochigi, Japan, **4** Department of Comprehensive Pathology, Graduate School, Tokyo Medical and Dental University, Tokyo, Japan, **5** Division of Diagnostic Pathology, Shizuoka Cancer Center, Nagaizumi, Shizuoka, Japan, **6** Department of Medical Genomics, Graduate School of Medicine, University of Tokyo, Tokyo, Japan

Abstract

The promising results of anaplastic lymphoma kinase (ALK) inhibitors have changed the significance of ALK fusions in several types of cancer. These fusions are no longer mere research targets or diagnostic markers, but they are now directly linked to the therapeutic benefit of patients. However, most available tumor tissues in clinical settings are formalin-fixed and paraffin-embedded (FFPE), and this significantly limits detailed genetic studies in many clinical cases. Although recent technical improvements have allowed the analysis of some known mutations in FFPE tissues, identifying unknown fusion genes by using only FFPE tissues remains difficult. We developed a 5′-rapid amplification of cDNA ends-based system optimized for FFPE tissues and evaluated this system on a lung cancer tissue with *ALK* rearrangement and without the 2 known ALK fusions EML4-ALK and KIF5B-ALK. With this system, we successfully identified a novel ALK fusion, KLC1-ALK. The result was confirmed by reverse transcription-polymerase chain reaction and fluorescence *in situ* hybridization. Then, we synthesized the putative full-length cDNA of *KLC1-ALK* and demonstrated the transforming potential of the fusion kinase with assays using mouse 3T3 cells. To the best of our knowledge, KLC1-ALK is the first novel oncogenic fusion identified using only FFPE tissues. This finding will broaden the potential value of archival FFPE tissues and provide further biological and clinical insights into ALK-positive lung cancer.

Citation: Togashi Y, Soda M, Sakata S, Sugawara E, Hatano S, et al. (2012) KLC1-ALK: A Novel Fusion in Lung Cancer Identified Using a Formalin-Fixed Paraffin-Embedded Tissue Only. PLoS ONE 7(2): e31323. doi:10.1371/journal.pone.0031323

Editor: Anthony W.I. Lo, The Chinese University of Hong Kong, Hong Kong

Received October 17, 2011; **Accepted** January 5, 2012; **Published** February 8, 2012

Funding: This work was supported in part by Grants-in-Aid for Scientific Research from the Ministry of Education, Culture, Sports, Science, and Technology of Japan as well as by grants from the Japan Society for the Promotion of Science; the Ministry of Health, Labor, and Welfare of Japan; the Vehicle Racing Commemorative Foundation of Japan; the Princess Takamatsu Cancer Research Fund; and the Uehara Memorial Foundation. The funders had no role in study design, data collection and analysis, decision to publish, or preparation of the manuscript.

Competing Interests: The authors have declared that no competing interests exist.

* E-mail: kentakeuchi-tky@umin.net

Introduction

Anaplastic lymphoma kinase (ALK) is a receptor tyrosine kinase that was discovered in anaplastic large-cell lymphoma (ALCL) in the form of a fusion protein, NPM-ALK [1,2]. The formation of a fusion protein with a partner through chromosomal translocations is the most common mechanism of ALK overexpression and ALK kinase domain activation. Recent promising results of clinical trials with an ALK inhibitor, crizotinib, have changed the significance of ALK fusions in lung cancer [3,4,5,6], inflammatory myofibroblastic tumors (IMTs) [7], and ALCL [8]. ALK fusions are no longer mere research targets or diagnostic markers and are now directly linked to the therapeutic benefit of patients.

In lung cancer, 3 fusion partners of ALK have been reported—EML4, TFG, and KIF5B—although the presence of TFG-ALK in lung cancer has not yet been proven with histopathological evidence [9,10,11]. In addition to lung cancer, ALK has further been found to generate fusions in ALCL (fused to NPM, TPM3, TPM4, ATIC, TFG, CLTC, MSN, MYH9, or ALO17) [1,2,12,13,14,15,16,17,18,19], IMT (TPM3, TPM4, CLTC, CARS, RANBP2, ATIC, or SEC31A) [19,20,21,22,23,24], ALK-positive large B-cell lymphoma (CLTC, NPM, SEC31A, or SQSTM1) [25,26,27,28], and renal cancer (VCL, TPM3 or EML4) (Table 1) [29,30]. In addition to TFG-ALK in lung cancer, some ALK fusions have been reported without histopathological evidence: TPM4-ALK in esophageal squamous cell carcinoma [31,32] and EML4-ALK in colon and breast carcinomas [33].

Anti-ALK immunohistochemistry played an important role in identifying these ALK fusion partners. Several ALK fusions exhibit a characteristic staining pattern in anti-ALK immunohistochemistry because the subcellular localization of ALK fusion proteins depends on the fusion partner. For example, NPM-ALK, which is the most common fusion in ALK-positive ALCL (85%), exhibits a nuclear and cytoplasmic staining pattern because the heterodimer of NPM and NPM-ALK localizes in the nucleus and the homodimer of NPM-ALK in the cytoplasm; CLTC-ALK exhibits a cytoplasmic granular pattern because it localizes in the small vesicles. If a tumor exhibits an unrecognized anti-ALK staining pattern, the patient may have a novel fusion partner. In addition to the difference in subcellular localization, the difference in staining intensity is a key to identifying novel partners. EML4-ALK is hardly stained by conventional anti-ALK immunohistochemistry [11,34]. To overcome this limitation, we developed the intercalated antibody-enhanced polymer (iAEP) method, which moderately increases

Table 1. ALK fusion partners.

Reported year	Partner	Locus	ALK+ALCL	ALK+LBCL	IMT	NSCLC	RCC
1994	NPM	5q35.1	+	+			
1999	TPM3	1p23	+		+		+
1999	TFG	3q12.2	+			+*	
2000	ATIC	2q35	+		+		
2000	TPM4	19p13	+		+		
2001	CLTC	17q23	+	+	+		
2001	MSN	Xp11.1	+				
2002	ALO17	17q25.3	+				
2003	MYH9	22q13.1	+				
2003	RANBP2	2q13			+		
2003	CARS	11p15			+		
2006	SEC31A	4q41		+	+		
2007	EML4	2p21				+	+
2009	KIF5B	10p11.22				+	
2011	SQSTM1	5q35.3		+			
2011	PPFIBP1	12p11			+		
2011	VCL	10q22.2					+
Present study	KLC1	14q32.1				+	

*Histopathological evidence is lacking. Abbreviations: ALCL, anaplastic large cell lymphoma; LBCL, large B-cell lymphoma; IMT, inflammatory myofibroblastic tumor; NSCLC, non-small cell lung carcinoma; RCC, renal cell carcinoma.

doi:10.1371/journal.pone.0031323.t001

sensitivity in the immunohistochemical detection system, and EML4-ALK was consistently stained with this method [11]. This indicated that a tumor that is positively immunostained for ALK only by a sensitive immunohistochemistry method but not by conventional methods may harbor a novel ALK fusion. Based on this hypothesis, we successfully identified PPFIBP1-ALK in 2 IMT cases that were positive in anti-ALK immunohistochemistry only when stained by the iAEP method [35].

Anti-ALK immunohistochemistry may thus be useful to detect candidate tumors for a novel ALK fusion. However, to identify the fusion partner, other molecular techniques are usually required such as 5′-rapid amplification of cDNA ends (5′-RACE) or inverse reverse-transcription polymerase chain reaction (RT-PCR). To the best of our knowledge, no novel oncogenic fusions have been discovered using formalin-fixed paraffin-embedded (FFPE) tissues only because nucleic acids extracted from FFPE tissues are severely degraded during the fixation process. In the present study, we developed a 5′-RACE method optimized for *ALK* fusion partner detection that was applicable to FFPE tissues and identified a novel fusion, kinesin light chain 1 (KLC1)-ALK, in lung cancer by using only an FFPE tissue.

Methods

Materials

A FFPE tissue block of pulmonary adenocarcinoma in situ, nonmucinous (formerly called bronchioloalveolar carcinoma) [36], which was excised from a 47-year-old female patient was used [37]. This carcinoma was negative for EML4-ALK and KIF5B-ALK, although the presence of *ALK* rearrangement was confirmed by anti-ALK iAEP immunohistochemistry and a split fluorescence in situ hybridization (FISH) assay for ALK (hereafter referred to as the unknown ALK fusion-positive case) (Figure 1) [37]. Two FFPE tissue blocks of ALK-positive tumor cases were also employed, for which the presence of EML4-ALK or KIF5B-ALK had already been confirmed. Total RNA was extracted from each FFPE tissue with the use of the RecoverAll™ Total Nucleic Acid Isolation Kit for FFPE (Applied Biosystems Japan, Tokyo, Japan). The ages of the 3 FFPE blocks used (time from FFPE tissue production to RNA extraction) were 65, 40, and 51 months for the unknown ALK fusion-positive case, EML4-ALK, and KIF5B-ALK, respectively. Written informed consent was obtained from each patient. The study was approved by the institutional review board of the Shizuoka Cancer Center (approval ID 22-J132-22-1) and the Japanese Foundation for Cancer Research (approval ID 2010-1011).

Modified 5′-RACE for ALK fusions applicable to FFPE tissues

5′-RACE was performed with the SMARTer RACE cDNA Amplification Kit (Clontech) according to the manufacturer's instruction with minor modifications. In brief, instead of the primers included in the kit, ALK-3242R (5′-CTCAGCTTG-TACTCAGGGC-3′) was used for cDNA synthesis. The cDNA was subjected to 5′-RACE PCR using PrimeSTAR HS DNA Polymerase (TaKaRa) and the following primers: Universal Primer A Mix of the kit and ALK-3206R (5′-ATGGCTTG-CAGCTCCTGGTGCTT-3′). The PCR condition consisted of 5 cycles at 94°C for 30 s and 72°C for 3 min; 5 cycles at 94°C for 30 s, 70°C for 30 s, and 72°C for 3 min; and 30 cycles at 94°C for 30 s, 68°C for 30 s, and 72°C for 3 min.

FISH

FISH analysis of fusion genes was performed with DNA probes for KLC1 and ALK. Unstained sections (4-μm thick) were subjected to hybridization with an ALK-split probe set (Dako, Tokyo, Japan) or with bacterial artificial chromosome (BAC) clone-derived probes for ALK (RP11-984I21 and RP11-62B19)

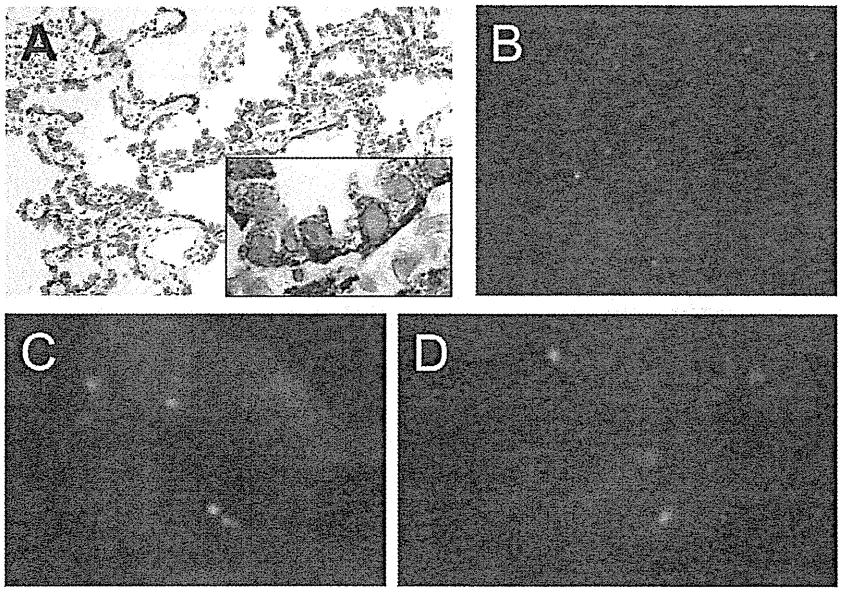

Figure 1. ALK-rearranged lung adenocarcinoma without EML4-ALK and KIF5B-ALK. Panel A shows the results of anti-ALK immunohistochemistry with the iAEP method on pulmonary adenocarcinoma in situ, nonmucinous. The staining pattern was diffusely cytoplasmic. The basal side of tumor cells was more strongly stained, indicating an uneven subcellular localization of KLC1-ALK protein. FISH analyses revealed that this case was positive in the split assay for *ALK* (Panel B: individual 5′- and 3′-signals are observed) and negative in *EML4-ALK* and *KIF5B-ALK* fusion assays (Panel C: *EML4*, red; *ALK*, green; Panel D: *KIF5B*, green; *ALK*, red).
doi:10.1371/journal.pone.0031323.g001

and KLC1 (RP11-186F6). Hybridized slides were then stained with DAPI and examined using a BX51 fluorescence microscope (Olympus, Tokyo, Japan).

Synthesis of the putative cDNA of *KLC1-ALK*

Two independent PCRs were performed using cDNA synthesized from a tumor tissue expressing KIF5B-ALK with the following primer sets: KLC1-NheI-M (5′-GCGCTAGCGAATGTATGACAACATGTCCAC-3′) and KLC1-bpR (5′-GTGCTTCCGGCGGTACACATCTACAGAACCAAACTC-3′), and ALK-bpF (5′-GGGAGTTTGGTTCTGTAGATGTGTACCGCCGGAAGC-3′) and ALK-EcoRI (5′-GATAGAATTCTCAGGGCCCAGGCT-3′). Then, the second PCR was performed using a 1/100 dilution of a mixture of the first PCR products as a template with the KLC1-NheI-M and ALK-EcoRI primers (Figure 2).

Transformation assay for *KLC1-ALK*

Analysis of the transforming activity of kinase fusions was performed as described previously [9,38,39]. A pMXS-based expression plasmid for each fusion was used to generate recombinant ecotropic retroviruses [40], which were then used individually to infect mouse 3T3 fibroblasts. The formation of transformed foci was evaluated after culturing the cells for 4 days. The same set of 3T3 cells was injected subcutaneously into nu/nu mice, and tumor formation was examined after 14 days. The animal experiments were approved by the animal ethics committee of Jichi Medical University (approval ID 1135).

Results

Identification of *KLC1-ALK* as a novel *ALK* fusion gene

Our modified 5′-RACE faithfully isolated cDNA fragments for *EML4-ALK* or *KIF5B-ALK* from known ALK- positive tumors (Supplementary Figure S1A and B). We then attempted to isolate cDNA fragments encompassing the fusion points from the unknown ALK fusion-positive case. Nucleotide sequencing of such 5′-RACE products revealed that 2 of 10 clones contained the 3′-terminus of exon 9 of *KLC1* (ENST00000348520) fused to the first nucleotide of exon 20 of *ALK* (ENST00000389048), indicating the presence of a novel fusion between *KLC1* and *ALK*. As this rearrangement constituted an in-frame fusion between the 2 genes, the full-length *KLC1-ALK* cDNA probably produces a protein of 984 amino acids containing an amino-terminal two-thirds of KLC1 and an intracellular region of ALK (Figure 3A). RT-PCR-mediated isolation of a fusion point successfully confirmed the in-frame fusion between the 2 messages (Figure 3A and B). Further, to confirm the genomic rearrangement responsible for the fusion, a fusion FISH assay was performed (Figure 3C). These results were consistent with the presence of t(2;14)(p23;q32.3), leading to the generation of *KLC1-ALK*.

Transforming potential of *KLC1-ALK*

The putative full-length cDNA of *KLC1-ALK* was synthesized from the frozen tissue with KIF5B-ALK fusion expression (Figure 2, Supplementary Figure S2), and was used to generate a recombinant retrovirus expressing the fusion protein with an amino-terminal FLAG epitope tag. Infection of 3T3 cells with the virus expressing KLC1-ALK readily produced multiple transformed foci in culture and subcutaneous tumors in a nude mouse tumorigenicity assay (Figure 4), confirming the potent transforming ability of KLC1-ALK.

Discussion

Here, by analyzing the FFPE tissues only, we successfully discovered a novel ALK fusion, KLC1-ALK. While snap-frozen materials sampled from biopsied or surgically removed specimens

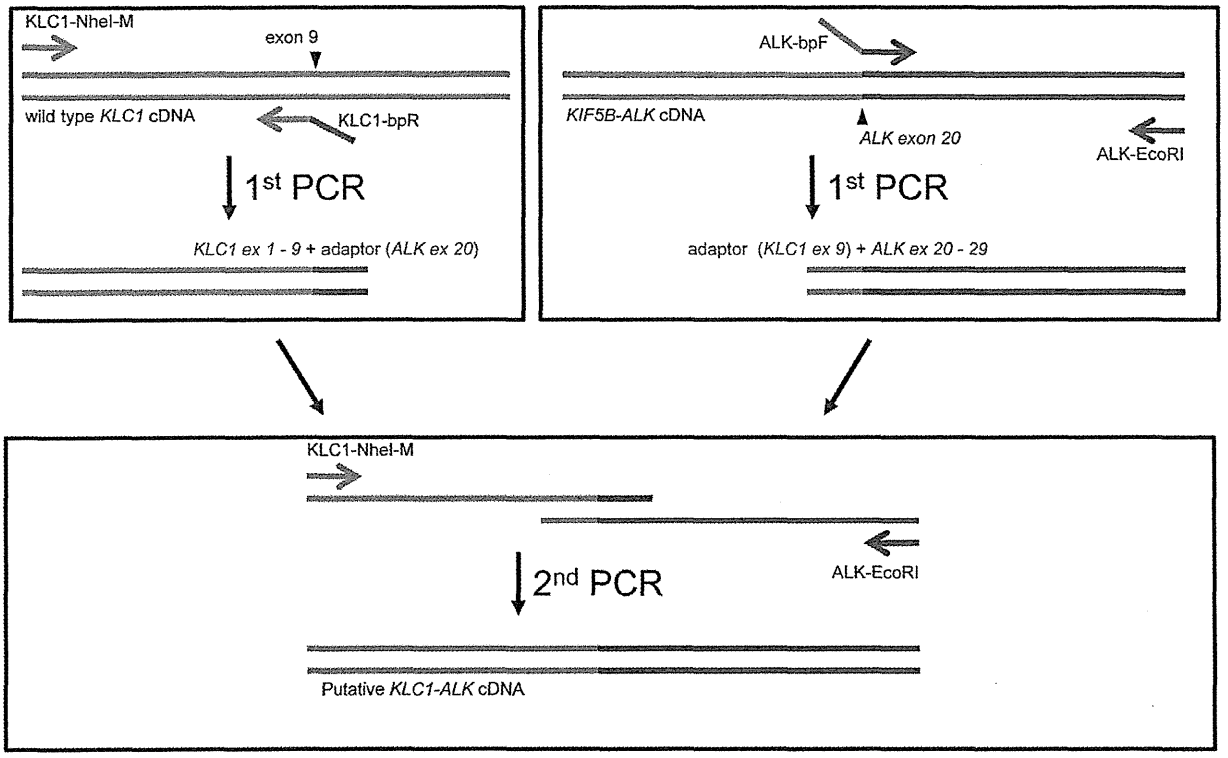

Figure 2. Synthesis of the putative KLC1-ALK full-length cDNA. Two first-round PCRs were performed separately using cDNA synthesized from a tumor tissue expressing KIF5B-ALK with the following primer sets: KLC1-NheI-M and KLC1-bpR, and ALK-bpF and ALK-EcoRI. KLC1-bpR and ALK-bpF had sequences downstream of the ALK break point (exon 20) and upstream of the KLC1 break point (exon 9) as adopter sequences, respectively. Then, the second PCR was performed using a 1/100 dilution of the mixture of the first PCR products as a template with primers KLC1-NheI-M and ALK-EcoRI. The first PCR products were annealed, extended with each other, and then amplified with the primers.
doi:10.1371/journal.pone.0031323.g002

can be used for various types of molecular analyses, they are not routinely sampled in most clinical settings. In contrast, FFPE specimens are usually produced, and histopathology diagnostic archives are an extremely large resource of FFPE tissues in ordinary diagnostic pathology laboratories. However, DNA and RNA extracted from FFPE tissues are severely degraded during formalin fixation and are usually not suitable for assays that need long DNA/RNA of high quality. Recent technical advances have allowed some analyses for known point mutations and known fusion genes, but it is still difficult to identify an unrecognized gene aberration using only an FFPE tissue.

In most *ALK* fusions, the break point of *ALK* is located within intron 19, and the fusion point in mRNA is typically the first nucleotide of exon 20. Therefore, if the primers for 5′-RACE are placed immediately downstream of the first nucleotide of *ALK* exon 20, such 5′-RACE may successfully isolate PCR products containing the partner gene sequence even using FFPE tissues. Based on this hypothesis, we established a 5′-RACE system for *ALK* fusions optimized for FFPE tissues. With this system, we identified a novel *ALK* fusion, *KLC1-ALK*. To the best of our knowledge, this is the first novel oncogenic fusion identified using only an FFPE tissue.

Caution, however, is needed. In some rare cases with *ALK* fusion, the break point of *ALK* fusion mRNA may not be at the 5′-end of exon 20. For example, in variant 4 of *EML4-ALK*, exon 14 of *EML4* is fused to an unknown sequence of 11 bp, which in turn is connected to nucleotide 50 of *ALK* exon 20 (E14;in-s11;del49A20) [38]. Our 5′-RACE system would not work on such a case because the reverse primer ALK-3206R corresponds to nucleotides 12–34 of *ALK* exon 20. Therefore, if our modified 5′-RACE fails to isolate fusion cDNAs from cases with a confirmed ALK rearrangement, other primer settings may be attempted.

Kinesin is a heterotetramer of 2 kinesin heavy chains and 2 kinesin light chains, and it moves on the microtubules towards their plus ends carrying various cargos. The heavy chains harbor the motor activity, whereas the light chains play roles in cargo binding and in modulating the activity and subcellular localization of the heavy chains. KLC1 binds to the kinesin heavy chains with an N-terminal domain and to various cargos via the tetratricopeptide repeat domains [41,42]. Of the 3 histopathologically confirmed ALK fusion partners in lung cancer, EML4 colocalizes with microtubules and may contribute to the stabilization of microtubules [43], KIF5B moves on the microtubules as a kinesin heavy chain [44], and KLC1 binds to kinesin heavy chains as a kinesin light chain. Therefore, it is interesting that all the 3 ALK fusions in lung cancer are likely to colocalize with microtubules.

The most frequent ALK fusion in lung cancer is EML4-ALK (4–7%) [9,38], and the second is KIF5B-ALK (0.5%) [11]. One case with TFG-ALK is reported [10]. KLC1-ALK may be rare but exists in lung adenocarcinoma, and the patients with this fusion are highly likely to benefit from ALK inhibitor therapy as do patients with other ALK fusions. The incidence may be low, but the significance of this fusion is very high from the perspective